Advances in Colloid and Interface Science 294 (2021) 102450

Contents lists available at ScienceDirect

Advances in Colloid and Interface Science

journal homepage: www.elsevier.com/locate/cis

Historical Perspective

Latest developments in nanofluid flow and heat transfer between parallel surfaces: A critical review

Mohammad Amani [b,*], Pouria Amani [c], Mehdi Bahiraei [d,*], Mohammad Ghalambaz [e,f], Goodarz Ahmadi [g], Lian-Ping Wang [h,i], Somchai Wongwises [j,k], Omid Mahian [a,l]

[a] School of Chemical Engineering and Technology, Xi'an Jiaotong University, Xi'an, Shaanxi 710049, China
[b] Department of Mechanical Engineering, Arak University of Technology, Arak, Iran
[c] School of Chemical Engineering, The University of Queensland, St Lucia 4072, Australia
[d] Faculty of Engineering, Razi University, Kermanshah, Iran
[e] Metamaterials for Mechanical, Biomechanical and Multiphysical Applications Research Group, Ton Duc Thang University, Ho Chi Minh City, Vietnam
[f] Faculty of Applied Sciences, Ton Duc Thang University, Ho Chi Minh City, Vietnam
[g] Department of Mechanical and Aeronautical Engineering, Clarkson University, Potsdam, NY 13699, USA
[h] Guangdong Provincial Key Laboratory of Turbulence Research and Applications, Center for Complex Flows and Soft Matter Research and Department of Mechanics and Aerospace Engineering, Southern University of Science and, Technology, Shenzhen 518055, Guangdong, China
[i] Department of Mechanical Engineering, University of Delaware, Newark, DE 19716, USA
[j] Fluid Mechanics, Thermal Engineering and Multiphase Flow Research Laboratory (FUTURE Lab.), Department of Mechanical Engineering, Faculty of Engineering, King Mongkut's University of Technology Thonburi, Bangmod, Bangkok 10140, Thailand
[k] National Science and Technology Development Agency (NSTDA), Pathum Thani 12120, Thailand
[l] Department of Mechanical Engineering, Center for Nanotechnology in Renewable Energies, Ferdowsi University of Mashhad, Mashhad, Iran

ARTICLE INFO

Available online 21 May 2021

Keywords:
Nanofluid
Heat transfer
Parallel plates
Squeeze flow
Concentric annulus

ABSTRACT

The enhancement of heat transfer between parallel surfaces, including parallel plates, parallel disks, and two concentric pipes, is vital because of their wide applications ranging from lubrication systems to water purification processes. Various techniques can be utilized to enhance heat transfer in such systems. Adding nanoparticles to the conventional working fluids is an effective solution that could remarkably enhance the heat transfer rate. No published review article focuses on the recent advances in nanofluid flow between parallel surfaces; therefore, the present paper aims to review the latest experimental and numerical studies on the flow and heat transfer of nanofluids (mixtures of nanoparticles and conventional working fluids) in such configurations. For the performance analysis of thermal systems composed of parallel surfaces and operating with nanofluids, it is necessary to know the physical phenomena and parameters that influence the flow and heat transfer characteristics in these systems. Significant results obtained from this review indicate that, in most cases, the heat transfer rate between parallel surfaces is enhanced with an increase in the Rayleigh number, the Reynolds number, the magnetic number, and Brownian motion. On the other hand, an increase in thermophoresis parameter, as well as flow parameters, including the Eckert number, buoyancy ratio, Hartmann number, and Lewis number, leads to heat transfer rate reduction.

Contents

* Corresponding authors.
E-mail addresses: amani.mohammad@gmail.com (M. Amani), mbahira@gmail.com (M. Bahiraei), mohammad.ghalambaz@tdtu.edu.vn (M. Ghalambaz).

https://doi.org/10.1016/j.cis.2021.102450
0001-8686/

Nomenclature

A	suction parameter
B	magnetic flux (T)
Bi	Biot number
Br	Brinkman number
C	concentration (vol% or wt%)
c_p	specific heat (J/K)
Da	Darcy number
D_B	Brownian diffusion coefficient
D_T	thermophoretic diffusion coefficient
Ec	Eckert number
E_h	electric parameter
h	distance between parallel surfaces (m)
M	Hartmann number/magnetization parameter
Hs	heat source parameter
k	thermal conductivity (W/m.K)
Kr	rotation parameter
N_B	Brownian motion parameter
N_{BT}	ratio of Brownian and thermophoretic diffusivities
N_T	thermophoretic parameter
Nu	Nusselt number
p	pressure (Pa)
Pr	Prandtl number
Q	heat source/heat sink (J)
q''	heat flux (W/m^2)
q_r	radiation heat flux (W/m^2)
R	viscosity parameter
Ra	Rayleigh number
Rd	radiation parameter
Re	Reynolds number
S	squeezing number
t	time (s)
T	temperature (K)
U_0	inlet velocity (m/s)
u, v, w	velocity components in the x-, y-, z-direction (m/s)
x, y, z	space coordinates

Abbreviation

EG	ethylene glycol
EO	engine oil
MHD	magnetohydrodynamic

Greek symbols

α_f	thermal diffusivity
β	coefficient of volumetric thermal expansion
β_1	Hall factor
β_R	mean absorption coefficient
ε	heat flux ratio
ζ	radius ratio
η	dimensionnels variable (= y/h)
λ	slip parameter
μ	dynamic viscosity (Pa.s)
ν	kinematic viscosity (m^2/s)
φ	nanoparticles volume fraction
ρ	density (kg/m^3)
σ	electrical conductivity (S/m)
σ_e	Stefan–Boltzmann constant
∇H	magnetic field gradient (T/m)
Ω	angular velocity (rad/s)

Subscripts

c	cold
f	base fluid
i	inner
m	mean
max	maximum
nf	nanofluid
o	outer
w	wall

1. Introduction

Fluids play a significant role in numerous industrial processes as heat carriers. The flow and heat transfer characteristics of fluids in thermal systems, ranging from car radiators to nuclear reactors, determine the performance of such systems. The performance of a thermal system can be improved through the enhancement of heat transfer. Heat transfer enhancement can result in more compact thermal equipment which saves energy and space and minimizes cost (Fig. 1). Various approaches classified as active and passive are widely used to improve heat transfer in many applications (Fig. 2). "Active" corresponds to the cases where an external power (force) is used for heat transfer enhancement, such as applying a magnetic field or creating vibration on the surface of a thermal device. On the other hand, "passive" represents techniques in which there is no external driver, such as extended surfaces (fins) and turbulators, for the increase of heat transfer. Using nanofluids instead of conventional liquids in thermal systems is also a passive technique for heat transfer improvement.

Fig. 1. Consequences of heat transfer enhancement.

One of the major limitations in heat transfer applications is the low thermal conductivity of conventional working liquids such as water, ethylene glycol (EG), and engine oil (EO). In recent years, nanofluids with a superior thermal conductivity compared to those of these base liquids have been introduced for improving the heat transfer performance in various applications [1–6]. Solid nanoparticles with various atomic structures have been used as additives to base liquids. The selection of nanoparticle type depends on the particular application as well as economic considerations.

In the literature, there are a number of review articles on nanofluids. For example, Ganvir et al. [7], Solangi et al. [8], and Suganthi and Rajan [9] summarized the studies performed on the thermophysical properties of nanofluids. Lomascolo et al. [10] presented a review of the recent experimental research on the conductive, convective, and radiative heat transfer in nanofluids. Considering the heat transfer in nanofluid flows, Hussein et al. [11] concentrated on the improvement of forced convection heat transfer using nanofluids, Haddad et al. [12] summarized the research on the natural convection heat transfer of nanofluids, and Pinto and Fiorelli [13] discussed the mechanisms responsible for improved heat transfer. In addition, Mahian et al. [14,15] reviewed recent developments in simulation methods and applications of nanofluid flows and discussed the challenges in the field.

There are also some reviews on modeling and simulation of nanofluid flows and heat transfer using different CFD approaches [16], numerical and semi-analytical approaches [17], and traditional and novel approaches such as single-phase effective media, Lattice Boltzmann methods, Eulerian-Lagrangian methods, mixture models, and thermal dispersion [18].

The most important thermophysical properties of nanofluids are thermal conductivity and dynamic viscosity [19–23]. The increased thermal conductivity of a nanofluid enhances the heat transfer rate, and the increase of dynamic viscosity intensifies the friction of fluid, thus demanding a higher pumping power. In this regard, a series of investigations were performed on the improvement of the thermal conductivity of nanofluids. Younes et al. [24] summarized the recent publications regarding the dispersion of nanoparticles to the base fluid to augment the thermal conductivity of nanofluids. Tawfik [25] presented a summary of experimental studies performed on the improvement of thermal conductivity of nanofluids and discussed the effects of nanoparticle size, shape, and concentration, as well as base fluid

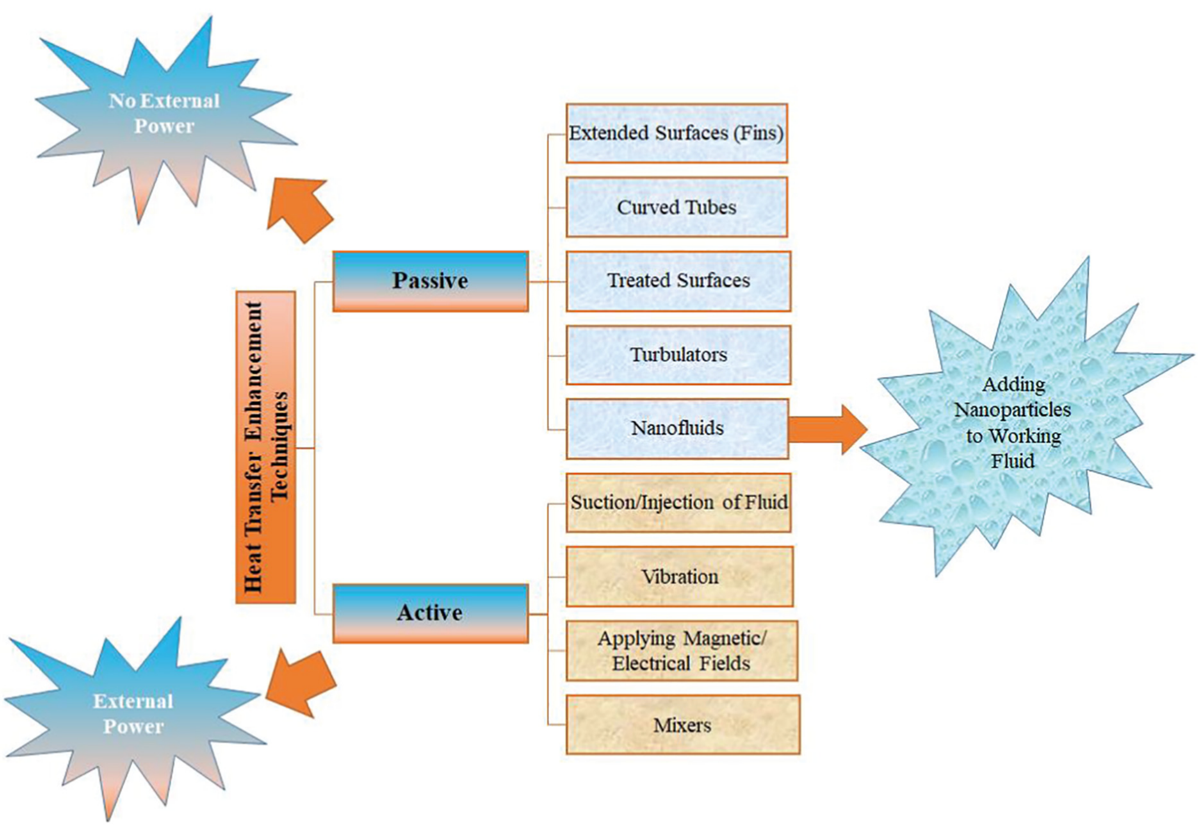

Fig. 2. A summary of techniques to enhance heat transfer. Using nanofluids is one of the passive techniques for enhancement of heat transfer.

type and temperature. Aybar et al. [26] described the mechanisms of thermal conductivity enhancement of nanofluids and summarized the models proposed in the literature. Regarding the rheological characteristics of nanofluids [27], the relevant experimental measurements [28] and the proposed dynamic viscosity models [29] were described. Azmi et al. [30] presented a comprehensive review of the research progress on improvement of the effective dynamic viscosity and effective thermal conductivity of nanofluids.

The hydrothermal performance of nanofluids in different industrial applications has also been reviewed. Kasaeian et al. [31] reviewed the recent application of nanofluids in porous media for thermal system applications. They described the effects of porosity, inertial coefficient, and permeability of porous media along with the influences of nanofluid parameters on the flow and heat transfer characteristics. Mahian et al. [32] and Kasaeian et al. [33] reviewed the influence of using nanofluids on the performance of solar water heaters, solar collectors, solar stills, solar cells, and thermal energy storage from environmental and economic points of view. In addition, they described the difficulties in utilizing nanofluids in solar energy systems. The application of nanofluids in heat exchangers [34] has been studied along with their behavior subject to magnetic fields in [35,36]. Amani et al. [37] presented a review of the influence of nanoparticles on the mass transfer performance and hydrodynamic behavior of liquid–liquid systems.

In recent years, many reviews of forced convection of nanofluid flows in tubes or natural convection in square and rectangular cavities have been published. However, only a few reviews in the literature were concerned with the evaluation of the flow and heat transfer of nanofluids in annuli. Togun et al. [38] reviewed the studies conducted on the heat transfer of fluids and nanofluids in various annular passages, including triangular, square, rectangular, elliptical, and circular configurations. Dawood et al. [39] summarized the investigations performed on the heat transfer analysis of fluids and nanofluids in concentric and eccentric annuli. Ahmed et al. [40] provided an overview of the thermal characteristics as well as applications of fluids and nanofluids in annuli.

Despite the extensive literature cited above, there is no review article that focuses on the thermal performance of nanofluid flow between parallel surfaces. Thus, in this paper, a comprehensive review is conducted on the hydrodynamic and thermal characteristics of nanofluids between parallel surfaces. The flow between parallel surfaces can be found in various types of heat exchangers that are used in different industries. The flow between parallel surfaces are classified into three groups as follows:

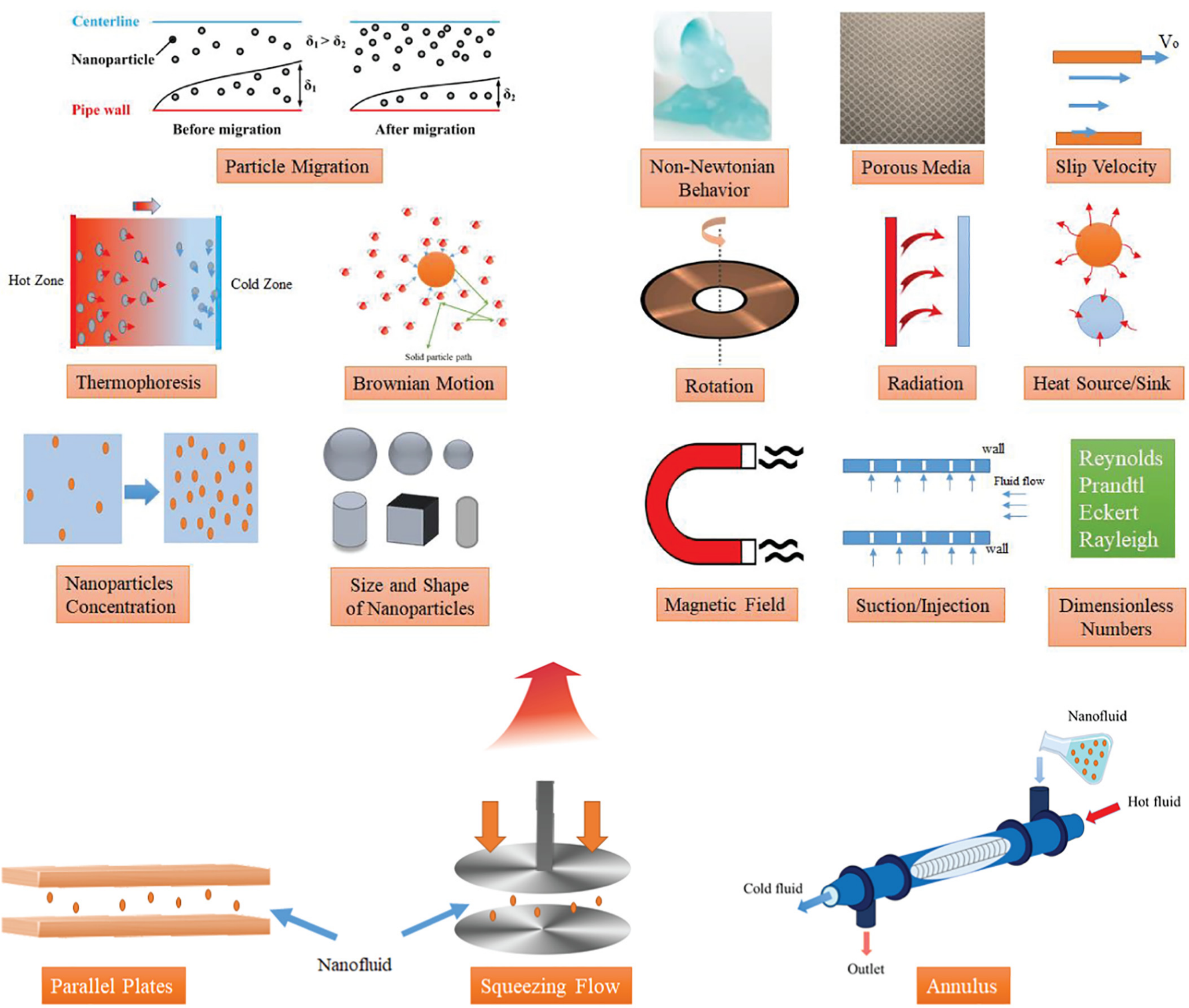

Fig. 3. An overview of physical phenomena and parameters governing the flow and heat transfer of nanofluids between parallel surfaces.

(I) Nanofluid flow between parallel plates/disks. Heat and fluid flow between two parallel plates/disks occur in many engineering applications such as cooling towers, micro-sized cooling systems, food processing, chemical processing equipment, lubrication systems, polymer processing, preparation, fog dispersion, and hydro-dynamical machines [40].
(II) Nanofluid squeezing film flow between parallel plates/disks. Recently, squeezing film flows between parallel plates/disks have been used extensively in engineering applications such as lubrication systems (e.g., load-bearing systems and flow of oil in bearings), compression and injection shaping, and food and polymer industries [41].
(III) Nanofluid flow through an annulus. Flow in a concentric annulus appears in cooling systems (e.g., electrical gas-insulated transmission lines and thermal insulations), thermal storage systems, and heat exchangers [42].

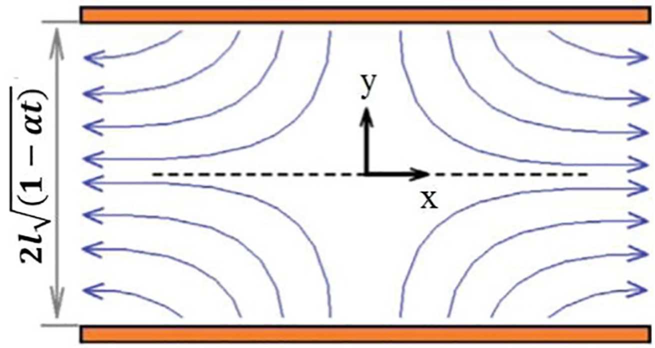

Fig. 5. Schematic of squeezing nanofluid flow between two parallel plates [49]. Here y represents the vertical coordinate, and l represents the initial position (at $t = 0$).

Due to a large number of investigations on the flow and heat transfer of different types of nanofluids between parallel surfaces, in this review, various sections are devoted to summarizing the effects of nanoparticle concentration, particle migration, magnetic field application, nanoparticle shape or type, different dimensionless numbers, slip velocity, presence of suction or blowing, a heat source or heat sink, use of non-Newtonian nanofluids, porous media, thermal radiation, rotating systems, heat flux ratio, radius ratio, and inclination angle on the heat transfer behavior of nanofluids. Fig. 3 schematically illustrates the aim of the present study. The present review paper mainly concerns the recent advances in these areas.

2. Mathematical formulation

The hydrodynamic and thermal performance of nanofluids between parallel surfaces are reviewed on the basis of different physical characteristics. The available literature suggests that the important configurations of the nanofluid flow between parallel surfaces are a) the flow between parallel plates, b) the squeezing flow between parallel plates, and c) the flow through concentric annuli.

An important group of studies of nanofluid flows between parallel surfaces investigates nanofluid flows between static parallel plates. A typical schematic of the flow of a heat-conducting nanofluid between two parallel plates is shown in Fig. 4. The position of the point (0; 0; 0) is kept unchanged by stretching the lower plate by two equal opposing forces. The top and/or the bottom plate may be set at a constant temperature (T) or a constant heat flux (q”) and/or can be permeable. In addition, the plates may be oriented horizontally or vertically. In most previous investigations, the nanofluid flow configuration was assumed to be two-dimensional to simplify the problem.

Squeezing flow is an important phenomenon in various industrial and mechanical processes related to flows between parallel surfaces. During squeezing flow, two parallel plates compress the material between them by moving in opposite directions, which spreads the flow in the radial direction. The squeezing film flow and thermal performance of nanofluids between two parallel plates have attracted considerable attention due to their potential industrial applications. Squeezing film flows are utilized in various technological applications such as food processing [43], transient loading of mechanical components [44], hydraulic and lubrication systems [45], polymer industries [46], molding of metals [47], and viscosity measurement by a viscometer [48]. A schematic of squeezing film flow is illustrated in Fig. 5. As can be seen in this case, the two plates are located at $y = \pm l\sqrt{(1-\alpha t)}$. When $\alpha > 0$, the plates are squeezed toward each other until they touch at $t = 1/\alpha$. The plates are separated when $\alpha < 0$. The nanofluid is considered to flow mainly along the x-axis, with its profile varying with the y-coordinate; the arrows in Fig. 5 signify the streamlines of nanofluid flow.

Flow through annuli is another configuration included in this review article, which has many applications in heat exchangers, nuclear reactors, gas turbines, and so forth. A typical schematic of flow through an annulus is shown in Fig. 6. This figure shows the nanofluid flow and heat transfer in the space between two horizontal tubes as an example of concentric annuli. The radii of the inner and outer tubes are R_i and R_o, respectively. The inner tube is adiabatic, and the outer tube is heated. Various investigations in the field of nanofluid flow and heat transfer in concentric annuli have been conducted, the majority of which are numerical studies that treat the nanofluids as an effective single-phase fluid.

Researchers have considered various parameters affecting the hydrothermal characteristics of nanofluid flow between parallel surfaces, including rotating systems, presence of magnetic fields, Brownian motion, thermophoresis, thermal radiation, and the presence of a heat source or heat sink. Taking into account these various effects, the

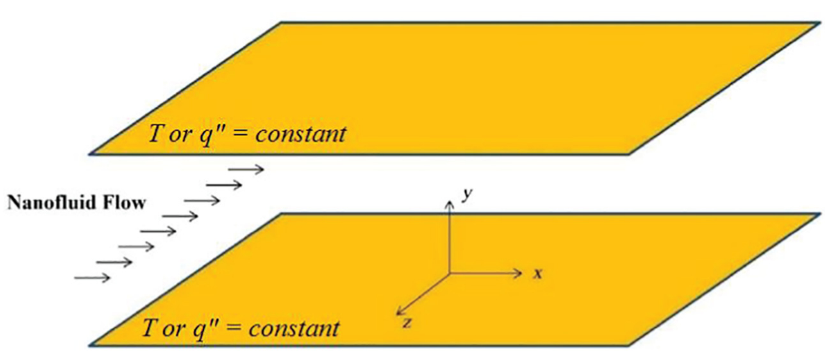

Fig. 4. Schematic of a heat conducting nanofluid flow between two parallel plates. The surfaces are at constant temperatures (T) or at constant heat fluxes (q”).

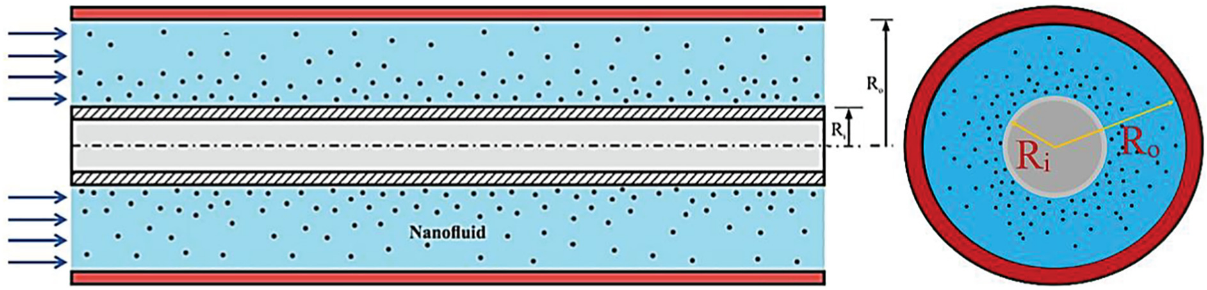

Fig. 6. Schematic of nanofluid flow through an annulus.

governing equations for flow, heat transfer, and mass transfer of nanofluids in a laminar flow regime can be expressed as follows [50]:

$$\frac{\partial u}{\partial x}+\frac{\partial v}{\partial y}+\frac{\partial w}{\partial z}=0 \tag{1}$$

$$\rho\left(u\frac{\partial u}{\partial x}+v\frac{\partial u}{\partial y}+2\Omega w\right)=-\frac{\partial p}{\partial x}+\mu\left(\frac{\partial^2 u}{\partial x^2}+\frac{\partial^2 u}{\partial y^2}\right)-\sigma B^2 u \tag{2}$$

$$\rho\left(u\frac{\partial v}{\partial x}+v\frac{\partial v}{\partial y}\right)=-\frac{\partial p}{\partial y}+\mu\left(\frac{\partial^2 v}{\partial x^2}+\frac{\partial^2 v}{\partial y^2}\right)-\beta\rho g(T_w-T) \tag{3}$$

$$\rho\left(u\frac{\partial w}{\partial x}+v\frac{\partial w}{\partial y}-2\Omega u\right)=\mu\left(\frac{\partial^2 w}{\partial x^2}+\frac{\partial^2 w}{\partial y^2}\right)-\sigma B^2 w \tag{4}$$

$$\begin{aligned}u\frac{\partial T}{\partial x}+v\frac{\partial T}{\partial y}+w\frac{\partial T}{\partial z}&=\frac{k}{\rho c_p}\left(\frac{\partial^2 T}{\partial x^2}+\frac{\partial^2 T}{\partial y^2}+\frac{\partial^2 T}{\partial z^2}\right)\\&+\left[D_B\left\{\frac{\partial C}{\partial x}\cdot\frac{\partial T}{\partial x}+\frac{\partial C}{\partial y}\cdot\frac{\partial T}{\partial y}+\frac{\partial C}{\partial z}\cdot\frac{\partial T}{\partial z}\right\}+\left(\frac{D_T}{T_c}\right)\left\{\left(\frac{\partial T}{\partial x}\right)^2+\left(\frac{\partial T}{\partial y}\right)^2+\left(\frac{\partial T}{\partial z}\right)^2\right\}\right]\\&+\frac{\mu}{\rho c_p}\left(2\left[\left(\frac{\partial u}{\partial x}\right)^2+\left(\frac{\partial v}{\partial y}\right)^2+\left(\frac{\partial w}{\partial z}\right)^2\right]+\left(\frac{\partial v}{\partial x}\right)^2+\left(\frac{\partial v}{\partial z}\right)^2+\left(\frac{\partial w}{\partial x}+\frac{\partial u}{\partial z}\right)^2\right)\\&-\frac{1}{(\rho c_p)_f}\frac{\partial q_r}{\partial y}+\frac{Q}{\rho c_p}T\end{aligned} \tag{5}$$

$$u\frac{\partial C}{\partial x}+v\frac{\partial C}{\partial y}+w\frac{\partial C}{\partial z}=D_B\left(\frac{\partial^2 C}{\partial x^2}+\frac{\partial^2 C}{\partial y^2}+\frac{\partial^2 C}{\partial z^2}\right)+\left(\frac{D_T}{T_c}\right)\left(\frac{\partial^2 T}{\partial x^2}+\frac{\partial^2 T}{\partial y^2}+\frac{\partial^2 T}{\partial z^2}\right) \tag{6}$$

Here u, v, and w represent the velocity in x, y, and z directions, respectively. C and T are the concentration and temperature, μ and ρ are the dynamic viscosity and the base fluid's density, k is the thermal conductivity, c_p denotes the nanofluid specific heat, and p represents the fluid pressure. The absence of $\partial p/\partial z$ in Eq. (4) indicates the presence of a net cross-flow along the z-axis. In the case of vertically oriented parallel surfaces, the term $-\beta\rho g(T_w-T)$ is added to Eq. (3), where β is the coefficient of volumetric thermal expansion and T_w denotes the wall temperature. Moreover, the term including $\frac{\mu}{\rho c_p}$ in Eq. (5) represents the effect of viscous dissipation. Though Eqs. (1)–(6) are expressed in the Cartesian coordinate system, the cylindrical coordinate is typically used for analyzing flows through an annulus.

In the following section, the parameters appearing in the governing equations are discussed in more detail.

- Rotation

When the domain of the fluid flow is rotating, the effect of rotation can be seen in the form of inertia in the fluid flow's momentum. Hatami et al. [50] studied the flow and heat and mass transfer of nanofluids in a rotating domain. The rotating domain was the space between two horizontal plates as depicted in Fig. 4, and the rotation was around the y-axis with a constant angular velocity Ω.

- Applied magnetic field

The applied magnetic field has important applications in physics, chemistry, and engineering. Magnetic nanofluids have many more applications in numerous scientific and engineering fields. In this case, a transverse magnetic field with an intensity of B is applied through the plates along the y-axis. The terms $\sigma B^2 u$ and $\sigma B^2 w$ on the right-hand side of the momentum equations (Eqs. (2) and (4)) reflect the influence of the applied magnetic field [51]. In these terms, σ is the electrical conductivity, and B represents the applied magnetic flux.

- Brownian motion and thermophoresis

Nanoparticle migration assumes that there is a slip velocity relative to the base fluid, which leads to the movement of nanoparticles inside the nanofluid. Buongiorno [52] concluded that the most significant slip mechanisms that have an influence on particle migration in nanofluids are Brownian motion and thermophoresis. In fact, the terms associated with the Brownian and thermophoretic diffusivities (D_B and D_T) on the right-hand side of the energy and concentration equations (Eqs. (5) and (6)) are the influences of Brownian motion and thermophoresis on the nanofluid flow [53].

- Thermal radiation

The term including q_r on the right-hand side of the energy equation (Eq. (5)) considers the influence of radiation heat flux, in which q_r can be determined according to the Rosseland approximation [54]. It should be noted that the thermal radiative properties, such as the absorption coefficient, are wavelength dependent.

Here, by the Rosseland approximation being taken into account, q_r can be expressed as follows:

$$q_r=-\left(\frac{4\sigma_e}{3\beta_R}\right)\left(\frac{\partial T^4}{\partial y}\right) \tag{7}$$

where β_R and σ_e are the mean absorption coefficient and Stefan–Boltzmann constant, respectively [54].

- Presence of heat source or heat sink

In the case of presence of a heat source or heat sink between parallel surfaces, the term including Q on the right-hand side of the energy equation (Eq. (5)) represents the effect of the heat source or heat sink [55]. In the following, the most recent studies on the flow and forced, natural, and mixed convection heat transfer of nanofluids in different configurations based on various characteristics are discussed, and the effects of various physical parameters are reviewed and investigated.

3. Effect of nanoparticle concentration

Various researchers have discussed the effect of nanoparticle concentration on the velocity profile of nanofluids between parallel plates [56–59]. Evaluation of velocity distribution along the *y*-direction for nanofluid flows revealed that velocities decrease with an increment in the nanoparticle content [57,59] as a result of an increase in the viscosity of the nanofluid. The maximum value of the velocity was seen in the central portion of the channel [57,60]. For the velocity along the *x*-direction, Khan et al. [57] performed a numerical analysis and observed an interesting behavior of the velocity profile. In the first half of the channel (i.e., $\eta\ (=y/h) < 0.5$), the velocity was found to decrease with an increase in nanoparticle concentration; however, an opposite behavior in the velocity was seen for the second half ($\eta > 0.5$), and an accelerated flow was evident. Following the previous two-dimensional studies, the velocity profile along the *z*-direction was studied numerically by Sheikholeslami et al. [59], and it was observed that when nanoparticle concentration increased, the thickness of the momentum boundary layer along the *z*-direction increased. Moreover, the irregular and random movements of particles were affected by the nanoparticle concentration. In particular, at high concentrations, peaks of the velocity component were observed.

Overall, the significant contribution of nanoparticles to the heat transfer improvement of the working fluid has been widely proved, and a direct relationship between the average Nusselt number (Nu) and nanoparticle concentration is observed in a majority of studies [50,54,56,57,59–65]. The main reason for this relationship is the increased thermal conductivity of the fluid and consequently higher energy transport between the wall and the fluid by the addition of nanoparticles. The thermal boundary layer thickness in the nanofluid is sensitive to the content of nanoparticles. Indeed, the increment of thermal conductivity is accompanied by greater values of thermal diffusivity, which increases the boundary layer thickness and reduces the nanofluid temperature gradient. A thinner thermal boundary layer on its own leads to a reduced Nu number. However, note that the Nu number is a function of the nanofluid thermal conductivity as well as the temperature gradient. By the addition of nanoparticles, the nanofluid thermal conductivity is significantly increased compared to that of the base fluid, thereby overcoming the negative impact of the reduction in the temperature gradient and resulting in a higher Nu number for concentrated nanofluids. In contrast, the numerical study of Singh et al. [66] revealed that considering the slip velocity, the heat transfer rate would be decreased at higher concentrations. In their paper, no reason is provided justifying why the Nu number varies inversely with nanoparticle concentration. In fact, the reason could be the decrease of mass transfer as well as reduction of Brownian motion's importance due to the intensification of viscosity owing to the concentration increment.

One of the points of interest is how the velocity profile of nanofluid flows varies against nanoparticle concentration under the squeezing condition. Although in some articles the influence of adding nanoparticles to the base fluid on the velocity boundary layer thickness is reported to be insignificant [66–71], there are studies that give different outcomes. For instance, Hayat et al. [72] disclosed a greater axial velocity profile for concentrated nanofluids away from the plates, while said profile was reduced near the plates. Singh et al. [66] reported that an increase in the values of nanoparticle fraction led to the velocity profile decrease near the lower plate, and after a fixed distance from the lower plate surface, it increased slightly. Acharya et al. [73] found that for $\eta < 0.42$, the velocity increases as nanoparticle concentration increases, but the trend is reversed for $\eta > 0.42$. A similar influence was reported for the movement of plates both toward and apart from each other. Most studies have covered the range of concentration $0 \le \varphi$ (vol%) ≤ 6, in which the velocity profile changes are not attributed to ranges of concentration considered in their studies. Changing the nanoparticle concentration affects the fluid temperature profile as well. It has been found that the nanofluid temperature possesses high values due to increasing nanoparticle concentration for the squeezing flow [67–69,72,74–78]. This effect occurs because the collision between particles and the plate's boundary surface and the collision of nanoparticles with each other are increased when two plates move toward each other. Therefore, the resulting friction increases the temperature within the fluid, particularly near the boundary regions. On the other hand, the opposite relationship is reported when two plates move apart [67–69,72,74–78]. Here, augmenting the nanoparticle content thickens the thermal boundary layer. It is reported that the influence of nanoparticle content on the thermal boundary layer thickness is insignificant when the Eckert number is low. Thus, the higher the Eckert number, the thicker the thermal boundary layer that is observed in concentrated nanofluids [74].

The effect of nanoparticle concentration on the flow and heat transfer attributes of nanofluids has also been examined in annuli. Huang et al. [79] studied the impact of the particle concentration on the hydrodynamics and free convection of a nanofluid in a 3D annulus. They reported that the flow strength and isotherms' deformation became weaker by increasing the particle concentration. Abbassi et al. [80] conducted a numerical simulation and observed that increasing both the Reynolds number (Re) and the nanoparticle concentration decreased the wall temperature in an annulus. Therefore, improved heat transfer can be achieved by augmenting the nanoparticle content, which intensifies chaos and movement of nanoparticles proportionately [81]. The enhancement of heat transfer by the addition of nanoparticles is found to be greater in laminar flow [80]. Accordingly, it has been found that the thermal conductivity is not the only reason for the enhancement of the Nu number and heat transfer, and various parameters such as slip condition, thermal boundary layer thickness, Brownian motion, and nanoparticles' chaotic movements are influential as well [81].

Abbasian Arani et al. [81] and Jafarimoghaddam and Aberoumand [82] experimentally studied the laminar thermal performance of Ag/oil and Cu/EG nanofluids in a concentric horizontal annulus. They obtained heat transfer improvement of more than 17% and 30% by dispersing 0.171 vol% Ag and Cu nanoparticles into the oil and EG, respectively. The increments in Nu number and heat transfer coefficient were observed by increasing the Peclet number. Khajeh Arzani et al. [83] performed an experimental analysis and considered the application of multi walls carbon nanotubes (MWCNTs) nanofluids as a coolant in a horizontal annulus in transient and turbulent flow regimes for possible use in heat exchangers utilizing an annular distributor. The highest heat transfer improvement of 22.4% was observed at a concentration of 0.1 wt% and $Re = 6807$. Heat transfer performance of the coolant at different heat fluxes revealed that the heat transfer performance is enhanced and the pressure drop decreases significantly with increases in circulation temperature. It is also noteworthy that the pressure drop and viscosity curves exhibit similar trends, which can be attributed to the direct relationship between pressure drop and viscosity [83].

In another study, Khajeh Arzani et al. [84,85] numerically evaluated the turbulent convection heat transfer of nanofluids consisting of functionalized graphene nano-platelet (GNP) nanoparticles dispersed in water and a mixture of EG and water in a horizontal concentric annular tube. The results showed increases of about 22% and 64% in the convective heat transfer coefficient at $Re = 17{,}000$ in the presence of 0.1 wt% and 0.2 wt% of the GNP/water and GNP/water-EG nanofluids, respectively. The results demonstrated that, for wide industrial applications, employing MWCNT and GNPs is highly beneficial due to their appropriate performance index and low friction factor and a weak increase in pressure drop. Fig. 7 schematically illustrates that both the increase of the Reynolds number and the increase of the volume fraction of nanoparticles enhance the heat transfer rate of a nanofluid flowing in an annulus.

Abbassi et al. [80,86] considered a nonuniform heat flux with a cosine shape applied on the inner tube and numerically investigated the thermal performance of the water-based TiO_2 and Al_2O_3 nanofluids in a vertical annulus (see Fig. 8). Because the heat flux has a cosine profile, the temperature will be maximized at a point above the middle of the

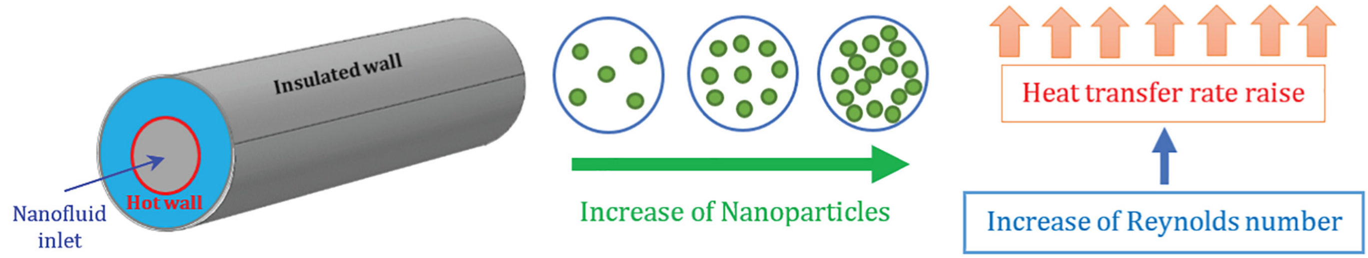

Fig. 7. The effect of using nanofluids in an annulus: the increased nanoparticles volume fraction and flow Reynolds number enhance the heat transfer rate.

heating region [80]. Regarding the evaluation of the *Nu* number along with the annulus height at different nanoparticle concentrations, the increasing effect of the nanoparticles on the heat transfer improvement was reported. The authors showed that increasing the flow rate and/or nanoparticle content leads to the higher temperature at the inner tube with more uniform distribution.

Aljabair et al. [87] examined the free convection within symmetrical and unsymmetrical annuli filled with a water–alumina nanofluid. They employed the stream function-vorticity formulation in the curvilinear coordinate for the solution of the equations that governed the heat transfer and fluid flow. Their findings indicated that the heat transfer was profoundly enhanced by the increment of the particle content and the *Ra* number.

Besides the variation of the *Nu* number, the value of the skin friction coefficient is frequently investigated due to its importance for understanding the flow behavior of nanofluids. Since the addition of nanoparticles in the working fluid increases its viscosity as well as the rate of energy exchange due to the irregular and random movement of particles, a direct relationship is frequently reported between the skin friction coefficient and nanoparticle content [58,62]. However, some studies, such as the work of Mahmoudi and Kandelousi [61], Khan et al. [57], and Sheikholeslami et al. [63], have argued for the existence of an inverse relationship between the skin friction coefficient and nanoparticle concentration. It should be noted that opposite trends may also be seen in squeezed film flow between two plates. For example, Rahimi-Gorji et al. [55] and Sheikholeslami and Domiri Ganji [88] argued that the presence of a heat source could result in an inverse relationship between the skin friction coefficient and nanoparticle concentration. Intensification of particle migration at higher concentrations can be an important reason for these outcomes. In reality, the particles migrate toward central regions with a greater intensity at higher concentrations, which reduces the viscosity near the walls. However, more investigations are also needed to discover the inconsistencies between the results of various studies.

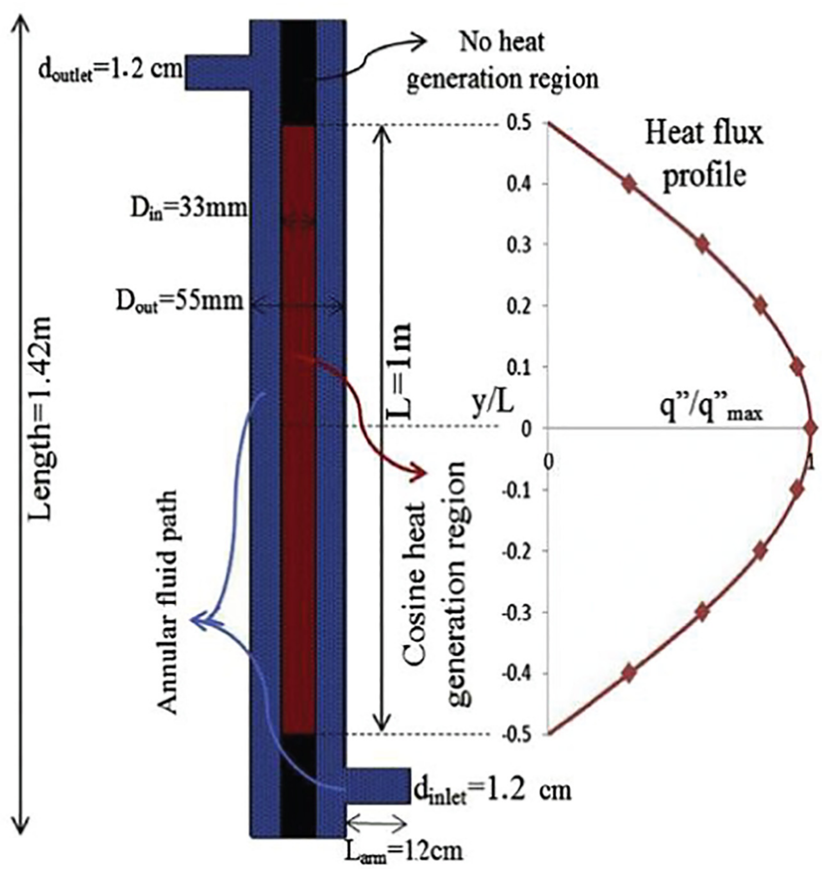

Fig. 8. Description of the annulus with cosine heat flux at the internal pipe surface [80].

Based on the observations, at low *Re* numbers, the increase in the friction factor by the addition of nanoparticles is more pronounced, indicating the essential role of Brownian motion in momentum transfer between particles and the base fluid at low flow rates. On the other hand, the significance of the influence of Brownian motion is reduced at high *Re* numbers, and higher velocity in turn has a more dominant role in increasing the friction factor at higher flow rates [84,85].

4. Effect of particle migration

It is known that in nanofluids the main slip mechanisms are Brownian motion and thermophoresis because of the extremely small size of nanoparticles. The Brownian motion is generated by the random movement of suspended particles due to the imbalance impacts of fluid molecules. The Brownian motion leads to a net mean mass flux, which is proportional to the concentration gradient of nanoparticles. Indeed, the Brownian motion tends to a uniform distribution of nanoparticles in the liquid.

The thermophoresis corresponds to the particle motion due to the temperature difference across the nanofluid (ΔT) that causes a nonuniform Brownian motion. That is, one side of the particle sees more impact due to the higher temperature than the other side does. This leads to a net force proportional to ΔT, which is termed thermophoretic force. In fact, this force intensifies the heterogeneity of the nanoparticle distribution with the development of higher concentration gradients in the base fluid [89]. This is attributed to the induction of nanoparticle migration in the opposite direction of ΔT from a warmer area to a colder area. Meanwhile, Brownian forces try to counterbalance the former effect by pushing particles in the opposite direction of the concentration gradient, which leads to the uniform dispersion of nanoparticles [89].

The Brownian motion is due to the collision of base fluid molecules with the nanoparticles, which results in the random movement of particles [90]. Two underlying mechanisms are responsible for the thermal conductivity improvement due to the Brownian motion of nanoparticles, including the direct contribution due to the particles diffusion and the indirect contribution due to the micro-convection around the particles [91]. Actually, the Brownian motion moves particles around randomly, and the particles also drag the fluid around in a random manner, generating a small turbulence-like effect. The Brownian diffusion increases when the temperature increases and the size of particles decreases; also, it increases with an increase in volume concentration of nanoparticles. However, recent studies argued that particle clustering plays a more important role in the thermal conductivity improvement in nanofluids than the latter effect [92–94]. The presence of particle clusters in nanofluids results in highly conductive pathways for the heat transport over long distances because the heat conduction by solid particles is much faster than that in the base liquid [95].

Thermophoresis, which is also known as thermodiffusion or the Soret effect, is the influence of the temperature gradient on isotopic or multicomponent mixtures of particles. The nanoparticles move from a higher to a lower temperature region due to ΔT in the base fluid. In this case, the nanoparticles migrate from the hot wall of the channel to the center core of the channel, which leads to a nonuniform particle concentration across the cross-section of the channel. The thermodiffusion can be regarded as "negative" and "positive" when particle migration occurs from a cold to a hot region and vice versa, respectively. Typically, the smaller or lighter particles show negative behavior, whereas the larger or heavier ones show positive thermophoretic behavior. The influences of thermophoresis are rather distinct from those of Brownian motion because the whole movements caused by the thermophoresis phenomenon are in opposite direction of the temperature gradient. Moreover, the relations of thermal conductivity induced by thermophoresis are independent of particle size. Fig. 9 illustrates the particle Brownian motion and thermophoresis phenomenon for the nanofluid flow in a channel with heated walls. As is seen, the thermophoresis tends to drive the nanoparticles away from the hot wall toward the cold regions, and hence the nanoparticles are accommodated in the central regions. The Brownian motion leads to a uniform nanoparticle distribution in a constant temperature fluid.

The Brownian motion is a zero mean stochastic process in a fluid at constant temperature. When there is a temperature gradient, the fluid molecular impact on the nanoparticle is no longer isotropic, and the corresponding Brownian motion develops a nonzero mean. The mean of anisotropic Brownian motion is referred to the thermophoresis effects. It should be pointed out that the Brownian diffusivity D_B disperses the particles and moves them from a region of high concentration to one

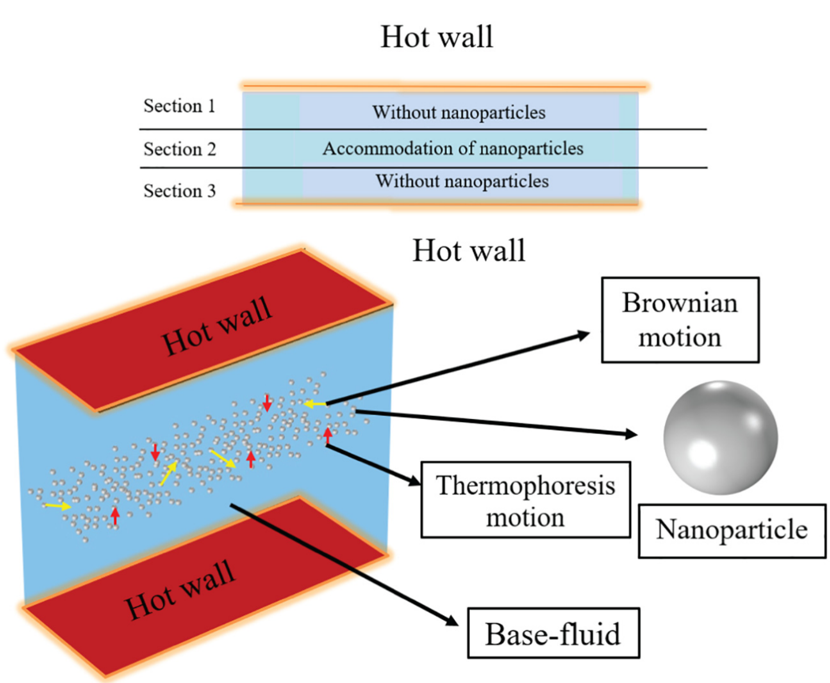

Fig. 9. Distribution of nanoparticles due to Brownian motion and thermophoresis effect in a channel with hot walls.

of low concentration. The thermophoresis diffusivity moves the particles from a region of high temperature to regions with low temperature. Therefore, the mutual effects of Brownian diffusion and thermophoresis diffusion should be considered for determination of nanoparticle migration in the presence of a temperature gradient. To evaluate the effect of particle migration on the nanofluid flow and heat transfer, the Brownian motion parameter (N_B) and thermophoretic parameter (N_T) are expressed in Eqs. (8) and (9) [53]. However, Brownian and thermophoretic parameters have a similar impact on temperature distribution and the *Nu* number [53,65,96–101]. This similarity means that the *Nu* number decreases with the increase of the temperature values of a nanofluid due to the increase of the temperature boundary layer thickness and the increase of the nanoparticles' kinetic energy. In some studies, the results were analyzed on the basis of the ratio of the Brownian motion parameter to the thermophoretic parameter ($N_{BT} = N_B/N_T$) to determine the impacts of thermophoretic and Brownian forces.

$$N_B = \frac{(\rho c)_p D_B (C_1 - C_2)}{(\rho c_p)_f \nu} \tag{8}$$

$$N_T = \frac{(\rho c)_p D_T (T_1 - T_2)}{(\rho c_p)_f \nu T_m} \tag{9}$$

The subscripts of *p* and *f* are associated with the nanoparticles and base fluid. The terms (C_1-C_2) and (T_1-T_2) represent the concentration difference and temperature difference in the domain, respectively. Also, as noted before, D_B and D_T are, respectively, the diffusion coefficients of Brownian motion and thermophoresis effects. Moreover, it has frequently been concluded that the concentration profile has an inverse relationship with the Brownian motion parameter [53,96–100], whereas with increasing N_B, Mohyud-Din et al. [65] observed a dual behavior for the concentration profile. It was observed that with the N_B increment, the concentration profile decreased at $0 \leq \eta \leq 0.5$ and started to increase at $\eta > 0.5$, indicating the unfavorable and favorable conditions for heat flow, respectively. In addition, the influence of the thermophoretic parameter on the concentration boundary layer thickness was not determined precisely. Sheikholeslami and Ganji [96], Mohyud-Din et al. [65], and Hatami et al. [50] showed that the concentration profile decreases with an increment of the thermophoretic parameter, whereas Sheikholeslami et al. [53,98], Sheikholeslami and Rokni [99], and Sheikholeslami and Ganji [100] reported an ascending trend for the concentration profile in terms of the thermophoretic parameter. It is noteworthy that the difference in particle size in the various studies can affect the observed results because thermophoresis is more significant for finer particles [101]. Moreover, Yang et al. [102] assessed the effect of N_{BT} on the hydrothermal characteristics of hybrid nanofluids. Two hybrid nanofluids consisting of Al_2O_3-TiO_2/water and Al_2O_3-ZrO_2/water were discussed in their analysis, which revealed that the decrease of N_{BT} in the case of Al_2O_3-TiO_2/water nanofluid and the increase of N_{BT} in the case of Al_2O_3-ZrO_2/water nanofluid resulted in the intensification of the *Nu* number with the penalty of a higher pressure drop. Later, Zhu et al. [103] studied the influences of particle migration on water-based TiO_2 and Al_2O_3 nanofluids between two parallel plates. They revealed that enhanced heat transfer performance was achieved at larger N_{BT}. This phenomenon can be attributed to the dependence of the shear stress on the walls and migration of nanoparticles on N_{BT}.

The impact of considering particle migration (due to the Brownian motion and thermophoretic parameters) when the flow of nanofluids between parallel plates is subject to squeezing has also received attention from researchers. The results of these investigations show that the Brownian motion and thermophoretic parameters have no considerable effect on the velocity profile, while they do have a great effect on temperature and nanoparticle concentration [104,105]. The summary of the results associated with the behavior of temperature distribution under the influence of Brownian motion and thermophoretic parameters reveals that by increasing the N_B and N_T, the temperature profile increases significantly [51,104–107]. It has been argued that the increase of the Brownian motion and thermophoretic parameters corresponds to a greater Brownian diffusion coefficient and thermophoretic force, which leads to a higher temperature distribution; accordingly, with an increase in N_B, temperature distribution would fall rapidly [108]. Furthermore, evaluating the variation of N_B and N_T with the concentration distribution for squeezing flow of nanofluids between parallel impermeable plates shows that the increase of N_B and the decrease of N_T lead to the increase of the concentration profile [51,105,106,109,110]. The concentration profile varies proportionately with N_B because the Brownian motion represents the effective movement of nanoparticles from the plates to the base fluid. On the other hand, the decreasing impact of N_T can be attributed to the movement of particles in the opposite direction of the temperature gradient. Meanwhile, investigating the effects of N_B and N_T on the concentration gradient of squeezing nanofluid flow between parallel permeable plates in the presence of suction and blowing revealed some different behaviors. It was concluded that with increasing N_B and decreasing N_T, the concentration profile decreases for suction flow. However, the concentration profile rises rapidly in the blowing case with increasing value of N_B and decreasing value of N_T [104,108].

The researchers also investigated the effect of particle migration in the nanofluid flow and heat transfer in annuli using N_{BT}. The

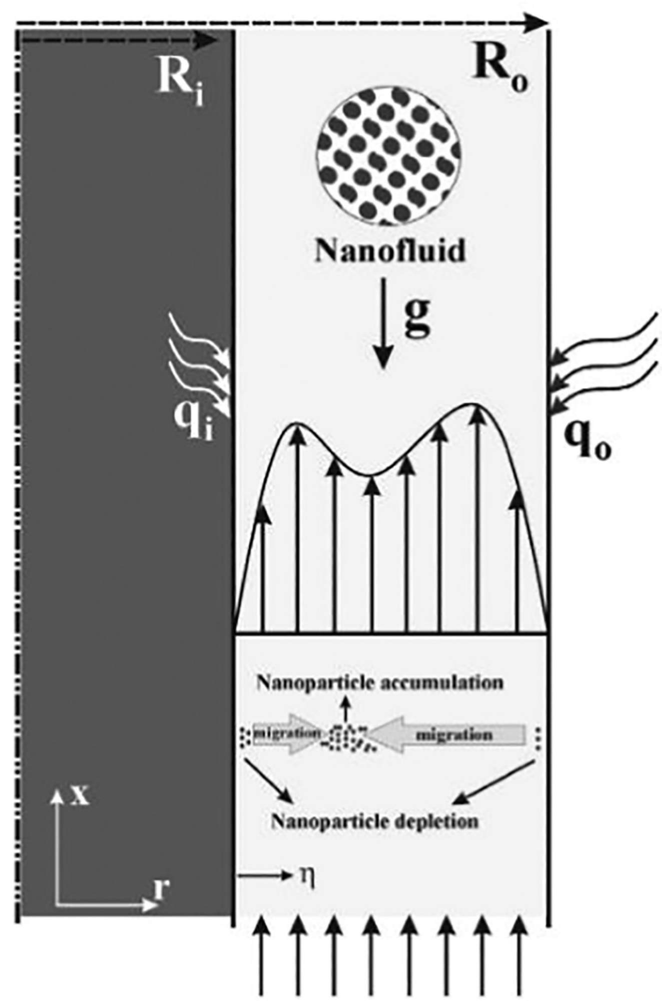

Fig. 10. Schematic of the physical problem [111].

concentration profile of nanoparticles becomes more uniform by increasing N_{BT} because of the decreased accumulation of nanoparticles near the cold wall and decreased migration of nanoparticles from the hot wall [89,111]. Migration of smaller particles is more intense, which leads to more uniform distribution of smaller nanoparticles. However, when N_{BT} is low, the domination of thermophoretic forces results in nonuniformity of particle concentration. In terms of velocity, the velocity profile of a nanofluid decreases near the hot wall in contrast to that near the cold wall, shifting the inflection point toward the cold wall due to the uniformity of nanoparticle concentration with increasing N_{BT}. In fact, when N_{BT} is low, a high concentration gradient of nanoparticles results in a higher velocity (due to smaller viscosity) near the hot wall and an inverse variation near the cold wall.

Apart from the velocity, the thermal conductivity of a nanofluid is a major function of N_{BT}, since the concentration of nanoparticles can significantly change the thermal conductivity of nanofluids [89,111]. Lower thermal conductivity on the cold side and increased thermal conductivity in the hot region are reported, indicating the rise in the temperature gradient on the cold side and an inverse trend on the hot side. Increasing N_{BT} has been found to make the temperature gradient uniform by homogeneously distributing the nanoparticles across the fluid. Near the hot wall, the reduced thermal conductivity decreases the heat transfer, while greater momentum transfer results in higher heat transfer. Therefore, the effective heat transfer rate is the result of the mutual effects of the Brownian motion and thermophoresis.

Zamani et al. [112] used the modified Buongiorno model [113], disregarding the dependency of thermophysical properties of nanofluid on the nanoparticle concentration. They considered the nanofluid flow under two boundary conditions: (I) the outer tube of the annulus had a constant temperature and the inner one was adiabatic, and (II) the outer tube was isolated and the inner one had a constant temperature. They revealed that the heat transfer characteristics for Cases I and II have distinct behaviors. For Case I, it was observed that the efficient thermal performance occurred at the lower values of N_{BT} and that said performance diminished as N_{BT} increased. For Case II, the thermal performance improved with the increment of N_{BT} and reached its highest value and then declined asymptotically to a constant value. Hence, it was expressed that the thermal performance reached its peak at an optimum value of N_{BT} in the range of $0.5 < N_{BT} < 1$. Malvandi and Ganji [111] employed a modified two-component heterogeneous model to study the mixed convection of an Al_2O_3/water nanofluid in a vertical annulus in which both the walls were heated uniformly. Fig. 10 shows the schematic of the physical problem. The authors showed that the direction of nanoparticle migration depended on the imposed thermal asymmetry. The heat transfer coefficient at the outer wall with higher heat flux decreased with increasing N_{BT}, particularly for the concentrated nanofluids. However, this coefficient at the inner wall with a lower heat flux increased with increasing N_{BT}. The total heat transfer coefficient increased with N_{BT} because of the greater contribution of the inner wall to the heat transfer process.

Hu et al. [114] concluded that the Brownian motion should be considered in the free convection of the nanofluid with regard to the density inversion phenomenon. The particle content and the radius ratio significantly influenced the flow and heat transfer features, whereas the particle size had a minor effect. The addition of the nanoparticles could have impaired or even overwhelmed the adverse impact of the density inversion phenomenon on the system thermal efficiency.

Finally, although considering the particle migration presents valuable information in the case of laminar flow, it is rather insufficient in the current form to determine nanofluid behavior under turbulent conditions or to transition to a turbulent regime. As a result, a modified technique should be introduced to clarify the physics of particle migration in turbulent and transition flow regimes. Future investigations should concentrate on nanoparticle motions as well as interactions between nanoparticles and turbulent eddies so that more efficient models can be provided for particle migration in turbulent flows of nanofluids. In addition, the migration of nanoparticles as a consequence of thermophoretic and Brownian motions should be examined by experimental studies as well.

5. Effect of applying magnetic fields

The influence of imposing magnetic fields on fluid behavior is of fundamental importance since it is the basis of various devices such as optical switches [115], cancer therapy and tumor elimination with hyperthermia [116], sterilizing devices [117], oil recovery from the underground reservoirs [118], bearings [119], generators [120], magnetohydrodynamic pumps [121], and so on. A typical illustration of an electrically conducting nanofluid flow between two parallel plates subject to a magnetic field perpendicular to the flow direction is given in Fig. 11. A uniform magnetic flux acts along the y-axis, and any induced magnetic field is neglected. In order to evaluate the effect of applying a magnetic field on the nanofluid flow and heat transfer, the Hartmann number/magnetization parameter (M) is represented in Eq. (10) [51]. Fig. 11 shows the effect of a downward uniform magnetic field on the flow of a nanofluid between two adiabatic plates. Here, the Brownian motion and magnetic field effects are the dominant nano-scale forces. The magnetic field drives the nanoparticles toward the bottom plate.

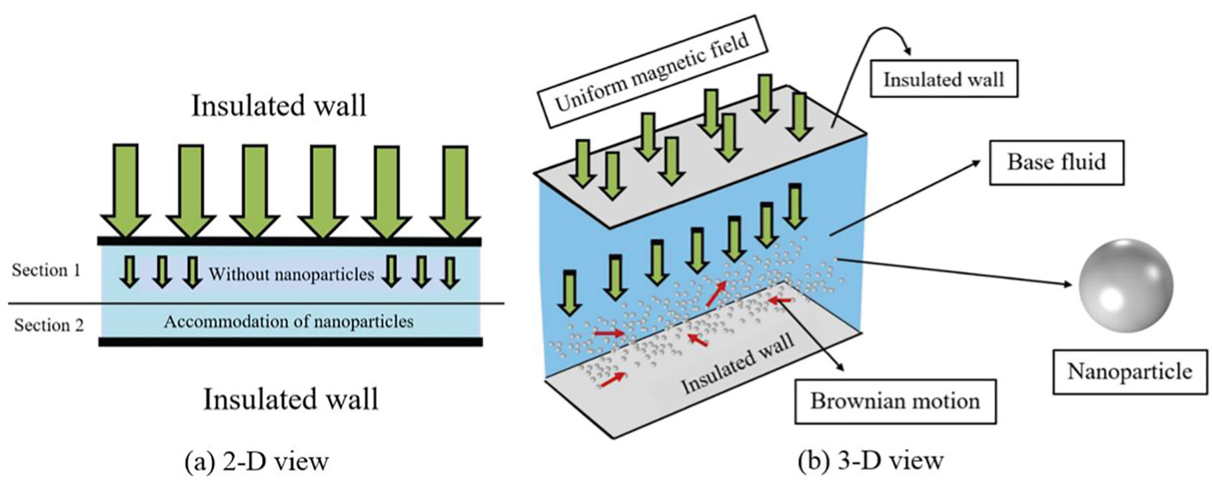

Fig. 11. The effect of a downward uniform magnetic field on the flow of a nanofluid between two adiabatic plates in the presence of the Brownian motion and magnetic field effect; (a) 2-D view and (b) 3-D view.

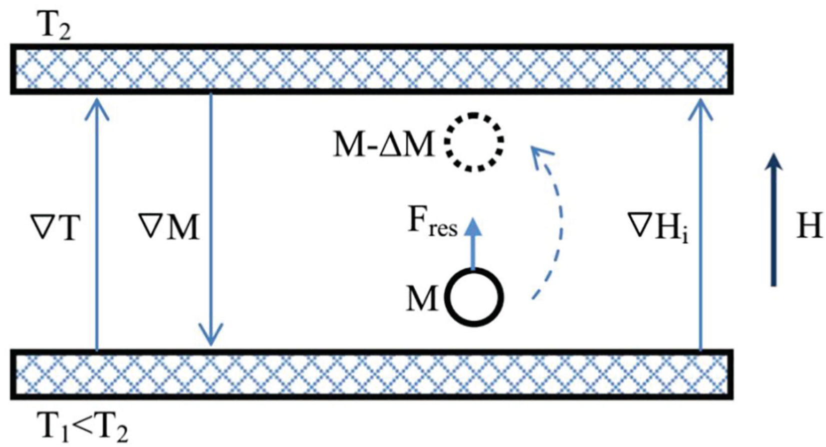

Fig. 12. Schematic of the presence of thermomagnetic convection which leads to displacement of the fluid particle, ΔMdenotes the reduction of magnetization adjacent to the hot wall in comparison with that near the cold wall [35].

The Brownian motion tends to disperse the nanoparticles back toward a uniform nanoparticle distribution in the fluid. As a result, the nanoparticles are accommodated in a region next to the bottom plate.

$$M = Bh\sqrt{\frac{\sigma_f}{\mu_f}} \tag{10}$$

where σ_f denotes the electrical conductivity of the fluid.

The natural convection of magnetic nanofluids is one area that has attracted much attention. In such cases, the temperature gradient and consequently the density difference result in the natural fluid motion due to the buoyancy force, which is known as the thermo-gravitational phenomenon. Besides the gravitational acceleration responsible for natural convection heat transfer, the fluid motion can also be controlled by a body force induced by magnetic fields. Moreover, a particular type of magnetic nanofluid is temperature-sensitive, such that its magnetization improves at lower temperatures. Therefore, the temperature gradient under a magnetic field could create a net magnetic driving force because of the formation of a nonequilibrium state in the fluid magnetization, thereby inducing fluid flow. This phenomenon is known as thermomagnetic convection, and a typical illustration of it is presented in Fig. 12. It can be seen that a vertical uniform magnetic field (H) and temperature gradient (∇T) exist collinearly in the nanofluid. According to the above discussion, the magnetization of the nanofluid near the hot wall with a temperature of T_2 is lower than that near the cold wall with a temperature of T_1, which results in a vertical variation in the magnetization of the nanofluid [35]. Thus, an inner magnetic field gradient (∇H_i) would be formed as follows:

$$\nabla H_i = H - D\nabla M \tag{11}$$

where D is the demagnetization factor and ∇Mrepresents the magnetization gradient. As can be seen in Fig. 12, the direction of ∇H_i is from the cold wall toward the hot wall. It is noteworthy that the resulting force (F_{res}) on the fluid element is applied in the direction of the displacement and has a destabilizing impact on the nanofluid layer, which induces a flow in the fluid. In fact, applying the temperature gradient results in a heterogeneously magnetized nanofluid due to the magnetization variation, which leads to the creation of heterogeneous body forces, known as Kelvin body forces in the magnetic nanofluids. It should be noted that the dashed lines in Fig. 12 show displacement of the fluid particles to a new location closer to the hot wall, while ΔMdenotes the reduction of the magnetization adjacent to the hot wall in comparison to that near the cold wall.

Many researchers have investigated the impact of applying magnetic fields on the nanofluid flow and heat transfer between parallel plates. According to their results, the magnitude of velocity in the x-direction decreases with an increase in the M parameter near the bottom wall and then increases slightly [53,57,63]. Moreover, researchers have observed that an increase in the M parameter lowers the velocity profiles in the y-direction [50,53,57,59,63,65,97–101], whereas it increases the profiles in the z-direction [63,65,97,98,101,122]. This observation is attributed to the significance of opposite forces to the flow (called Lorentz forces) caused by heightening the M parameter, which leads to inhibiting the movement of fluid in the boundary layer and increasing the friction force of the fluid. In magnetohydrodynamics (MHD) flows, the Lorentz force controls the vibration of the particles within the fluid. This force limits the flow velocity in the boundary layer and restricts fluid motion along the y-axis, and the transverse application of the magnetic field makes the velocity of the fluid more uniform, while another force called the Coriolis force reveals the reverse effect on the velocity along the z-direction.

In addition, the temperature distribution of nanofluid was represented as directly proportional to the magnetization parameter, and thus the Nu number improves with the decrement of this parameter due to the increase of the thermal boundary layer thickness [53,59,63,65,97,101]. In other words, the temperature distribution decreases for lower values of magnetization, M, and increases for larger values of M due to the dependence of the magnetization on the Lorentz force. Regarding the evaluation of the skin friction coefficient, researchers concluded that the intensification of a magnetic field leads to the increase of the skin friction coefficient's absolute values [53,57,59,63,65].

Rokni et al. [122] numerically studied the impacts of both a magnetic field and an electrical field on a Cu/water nanofluid flow between two parallel plates. A uniform magnetic flux and an electrical field ($E = E_0 xy$) acted along the y- and z-axes, respectively. They found that the Nu number was directly proportional to the electrical parameter ($E_h = E_0/B_0 ah$). The skin friction coefficient decreased as the electrical parameter increased. Mosayebidorcheh et al. [58] and Ali et al. [123] numerically studied the Couette flow of nanofluids under a magnetic field. The unsteady turbulent Couette flow and heat transfer of CuO/water nanofluids under a magnetic field considering the Hall effect were simulated by Mosayebidorcheh et al. [58]. The geometry consisted of two infinite horizontal plates, in which the upper plate moved with uniform velocity with respect to the stationary lower plate. They observed a linear relationship between the Nu number over the bottom wall and the Hall parameter ($m = \sigma_f \beta_1 B$). The Hall parameter is important in MHD Couette flows because the associated term initiates secondary flows along the z-axis. As the Hall parameter increased, velocity profiles were increased, thereby heightening the skin friction coefficient. The thickness of thermal boundary layers, however, was

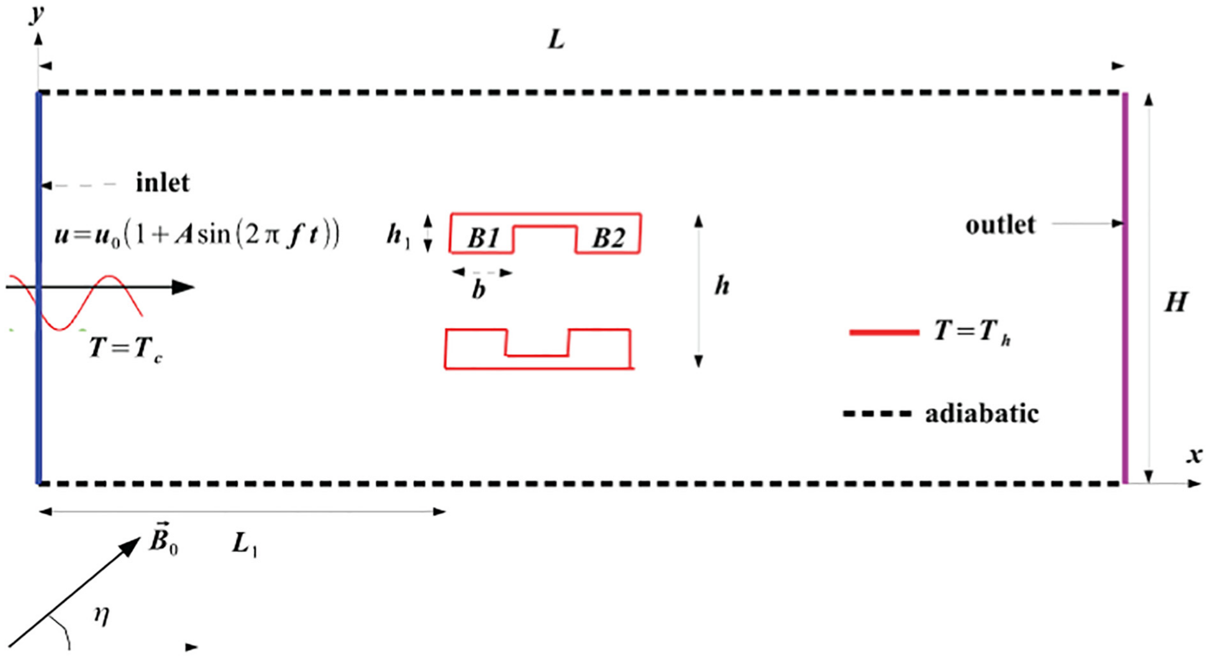

Fig. 13. The physical model under study [124].

decreased with an increasing Hall parameter. Ali et al. [123] analyzed the laminar Couette flow of nanofluids in a rotating system under a magnetic field and found that the *Nu* number was enhanced when the Hartmann number increased. The *M* parameter was observed to influence the primary velocity near the stationary plate and to retard the primary flow near the moving plate. The secondary flow was also observed to decrease when magnetic field strength was increased.

Selimefendigil and Öztop [124] investigated the forced convection of a pulsating nanofluid flow between parallel corrugated plates under an inclined magnetic field (see Fig. 13). Based on their observations, increments of the *Re* number, *Ha* number, magnetic inclination angle, and nanoparticle content enhance the heat transfer, whereas the corrugation wave parameters have an opposite effect on the heat transfer improvement.

Due to the important influence of applying a magnetic field to nanofluids to increase the heat and mass transfer [125–128], many researchers have also evaluated the characteristics of squeezing flow of nanofluids between parallel plates/disks in the presence of magnetic fields. The majority of their articles have considered a constant magnetic field, while some investigations have considered the flow under a variable time-dependent magnetic field with the intensity of $B(t) = B_0(1\text{-}\alpha t)^{-1/2}$ imposed perpendicular to the parallel plates/disks [51,55,66,70,71,73,88,109,129–134]. The squeezing flow of nanofluids between parallel plates under variable time-dependent magnetic fields is another type of problem, which is reviewed and discussed in this section.

Studies focusing on the effect of the *M* parameter on velocity profiles have revealed that as the magnetization parameter increases, the axial velocity is decreased for $\eta \le 0.4$ due to the Lorentz force, which hinders the fluid movement in the boundary layer area; for $\eta > 0.4$, however, the inverse effect is seen [51,55,66,71,73,88,130]. Furthermore, adverse pressure gradients are increased in the case of squeezing flow (when the two plates move toward each other) because of the reduced Lorentz force and the very close distance between the two plates in this condition. Note that a point of separation and backflow may occur whenever such forces act over a long time under this condition. On the other hand, the fluid velocity would be increased in newly created vacant spaces when the two plates move apart (to comply with the mass conversion). For this reason, an accelerated flow is evident for $\eta > 0.4$. Researchers observed that the radial velocity was inversely proportional to the magnetization parameter because the presence of a magnetic field defines the Lorentz force acting against the flow if the magnetic field is applied perpendicular to the direction of fluid flow [55,70,71,88,109,133,134]. Moreover, it was shown that the temperature distribution decreases with increasing *M* [51,55,66,71,73,88,133,134], while Dogonchi et al. [70] observed an opposite trend in a similar problem but in the presence of thermal radiation. Of course, it should be noted that the presence of thermal radiation results in a thicker thermal boundary layer and varies the *Nu* number, which can be the cause of this inconsistency. In addition, it is conceivable that the increase of the magnetization parameter leads to the increment of the skin friction coefficient in squeezing flows [51,55,66,70,73,88,107,129,133,135]. Furthermore, investigating the influence of the *M* parameter on the concentration profile revealed that the concentration profile is an increasing function of the magnetization parameter, and it can be the reason for the increase in the skin friction coefficient.

Investigation of the impact of magnetic fields on the nanofluid flow and heat transfer in concentric annuli is also of noticeable importance. The corresponding studies in this field [89,136–145] reveal that by applying a magnetic field, thermophoresis force tends to move particles from hotter to colder areas, resulting in the creation of a particle-free layer in the vicinity of the hot surface. Therefore, a concentrated region may be formed far from the heated wall. This local increase in nanoparticle concentration has been found to be more pronounced as the *M* parameter grows.

The magnetic parameter was used to explain the decrease of maximum velocity in the middle region of the fluid flow in annuli. The decrease owes to increased Lorentz force, which is a resistive-type force, on the velocity field caused by applying a magnetic field [139,141,143]. In other words, applying a magnetic field has been found to flatten the velocity profile because the nanoparticle concentration is greater in regions farther from the walls [140]. Consequently, the velocity gradient at the walls increases corresponding higher slip velocity due to moving the momentum at the core region of the annulus toward the pipe walls [143].

Focusing on heat transfer rate, researchers have found the average *Nu* number in annuli to be either an increasing function [142,143] or a decreasing function [89,137,138,144,145] of the *M* parameter. Firstly, arguments for the existence of a direct relation between the *M* parameter and the *Nu* number are discussed. Under a magnetic force, the rotation and movement of nanoparticles increase elongation in the orientation of the magnetic field, in which, therefore, nanoparticles would be aggregated in the magnetic field direction. This phenomenon has two distinct effects: (I) formation of pathways with lower thermal resistance and, in turn, high local thermal conductivity; and (II) greater interaction between aggregates and the base flow, which increases the energy and momentum transport, thereby yielding higher heat transportation. Moreover, it is clear that the magnetic field impact on the *Nu* number is more pronounced at lower concentrations [143]. Investigating the influences of the *M* parameter on the *Nu* number for various radius ratios revealed that higher heat convection inside the annulus could be obtained by increasing the radius ratio because of greater momentum exchange. Furthermore, at very high radius ratios, the nanoparticle movement is limited due to the high momentum transfer in the transverse direction of the annuli, and consequently the *Nu* number becomes almost independent of the *M* parameter as the radius ratio grows, while at low *M* values, a direct relationship is established between the *Nu* number and the *M* parameter [143].

Despite the articles mentioned above, there are cases where an inverse relation between the magnetization parameter and the *Nu* number has been observed. For instance, Selimefendigil and Oztop [138] investigated the effect of an inclined magnetic field on the MHD natural convection of a CuO/water nanofluid and found that when the magnetic inclination angle was increased and/or the *M* parameter was decreased, the local and average *Nu* numbers were enhanced. In fact, the observed disagreement for the *Nu* number changes in terms of the magnetization parameter compared with in the other studies can be due to the local redistribution of flow velocity inside the annulus with an increase of magnetic field strength, which locally decreases stream function in some parts. In effect, the displacement motion of the fluid weakens adjacent to the inner wall, which causes an indirect relationship between the *Nu* number and the *M* parameter. The rate of the heat transfer deterioration with a magnetic field became less effective for higher values of the *M* parameter. These researchers proposed that the magnetic field acts in a way to increase the local heat transfer for the upper part of the hot wall and to decrease the local heat transfer for the rest of the hot wall [138].

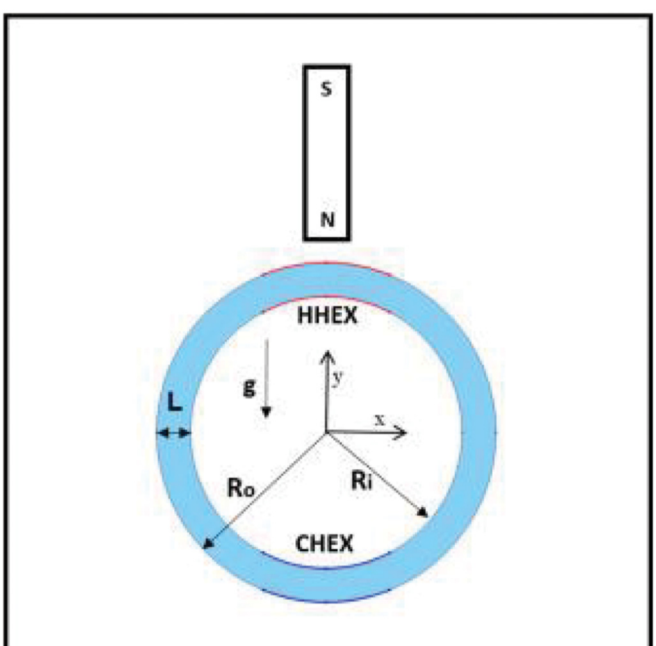

Fig. 14. Geometric description of the problem [147].

Evaluating mixed and natural convection of nanofluids in annuli under magnetic fields is another interesting topic for scholars. Malvandi et al. [144,145] numerically studied the mixed convection of Al_2O_3/water nanofluids in micro-annuli and revealed that inclusion of nanoparticles decreases the heat transport capacity of the working fluid in the presence of a magnetic field [144]. Also, they showed that heat transfer varies proportionately with the *M* parameter considering the dependency of thermophysical properties on the temperature [145], indicating the complexity of the heat transfer phenomenon under a magnetic field. Malvandi and Ganji [89] theoretically studied the natural convection of an Al_2O_3/water nanofluid in a vertical enclosure and declared that the temperature and concentration profiles are approximately insensitive to an applied magnetic field.

The nanoparticle size can also be an important factor affecting flow characteristics of nanofluids between parallel surfaces in the presence of magnetic fields. Bahiraei et al. [140] studied the effect of ferrohydrodynamics on the hydrothermal behavior of an Mn—Zn ferrite nanofluid inside an annulus. They observed that the heat transfer rate increased with particle enlargement in the attendance of a magnetic field, because of the significant dependence of the magnetic force on the size of particles such that the enlargement of the particles increases the magnetic force. Moreover, the rate of increase in the heat transfer was higher for larger particles since they have greater saturation magnetization. In other words, the particles reach their saturation magnetization in stronger magnetic fields.

Aboud et al. [146] studied the hydrodynamic features and mixed convective heat transfer of a copper–H_2O nanofluid within an annulus under a magnetic field. The annulus had an external rotating cylinder kept at a cool temperature, and an internal fixed cylinder kept at a warm temperature. The magnetic field critically affected the flow pattern. The mean *Nu* number was enhanced by reducing the Richardson number due to the improvement in the heat transfer because of the forced convection.

Dalvi et al. [147] studied the variation in the flow features due to the magnetocaloric response of the nanoparticles in a circular annulus. Their setup is shown in Fig. 14. Three different magnitudes of the remanent flux density (*Br*) and three different geometric structures were considered. A periodic clockwise flow rotation was observed in all cases, the frequency of which varied with either the geometric size or the remanent flux density.

Dogonchi and Hashim [148] evaluated the free convection and thermal radiation in the heat transfer of a nanofluid within an annulus. The enclosure included a wavy cylinder and a rhombus cavity exposed to a constant magnetic field. It was shown that the heat transfer amount diminished by elevating the aspect ratio in the absence of the *Ha* number. Furthermore, with the decrease of the aspect ratio, the flow space in the cavity became more extensive.

It should be noted that the thermophysical properties of nanofluids are noticeably dependent on the kind and state of the employed magnetic field, and so models of properties for nanofluids under different magnetic fields in a single-phase simulation can be different from each other. Consequently, more essential care should be given as mathematical models of thermophysical properties are used in numerical solutions. Moreover, the studies on the flow of nanofluids in parallel plates can be extended to devices whose operation is based on the thermomagnetic phenomenon because such equipment can have significant applications in the area of heat transfer engineering, such as cooling of new electronic components. In addition, with more advances in ferromagnetic materials possessing higher magnetization and pyromagnetic factors, magnetic nanofluids will show noticeable practical applications in many areas related to thermal engineering and management. Meanwhile, it is expected that the magnetoviscous impact on nanofluid convection will be considered in detail in future investigations.

Table 1
Types of nanoparticles employed for the nanofluid flow between parallel surfaces.

Authors	Nanoparticles under study	Geometry	Main remarks
Aly and Sayed [68]	Ag Cu Al_2O_3 TiO_2 SiO_2	Parallel plates	Type of nanofluid is an important factor for heat transfer enhancement as titania and silver give the highest and lowest value of the temperature, respectively.
Pourmehrban et al. [75]	Cu Ag Al_2O_3 TiO_2	Parallel plates	Selecting silver as nanoparticle leads to obtain the highest values of Nusselt number.
Azimi and Mirzaei [76], Azimi et al. [78]	GO Al_2O_3 TiO_2 Ag	Squeezing Flow between Parallel plates	The maximum amount of the Nusselt number is obtained by choosing silver as the nanoparticles.
Kandasamy et al. [131,132]	Cu Al_2O_3 SWCNT	Squeezing Flow over a porous sensor surface	The sphere shape nanoparticle in SWCNTs has more desirable improvement on heat transfer.
Bahiraei et al. [149]	Al_2O_3	Narrow annulus	Using smaller particles caused a greater heat transfer coefficient.
Alawi et al. [150]	Al_2O_3 CuO SiO_2 ZnO	Horizontal Concentric Annuli	The nanofluid with the SiO_2 particles has the highest Nusselt number and pressure drop compared with other nanofluid types.
Togun and Kazi [151,152]	TiO_2 CuO $Al2O_3$	Annular concentric pipe	The maximum heat transfer coefficient is observed with Al_2O_3.
Pena et al. [153]	AlN TiO_2	vertical annuli	Nanofluids with TiO_2 nanoparticles showed better heat transfer improvements than AlN.

6. Effect of nanoparticle shape or type

Since the thermophysical properties of different types of nanoparticles are different, the use of various types of nanoparticles leads to different outcomes. Table 1 illustrates the types of nanoparticles employed for the nanofluid flow between parallel surfaces. For instance, considering the work of several groups of researchers [68,75–78] focusing on the unsteady squeezing flow of different types of nanofluids consisting of GO, Cu, Ag, Al_2O_3, TiO_2, and SiO_2 nanoparticles between parallel plates, one can conclude that the dispersion of Ag nanoparticles in water can lead to a higher *Nu* number. Moreover, the Cu/water nanofluid had a more uniform temperature profile for the same Eckert number value and nanoparticle concentration. In other studies, Kandasamy et al. [131,132] investigated the effect of nanoparticle shape (i.e., sphere and cylinder) on an MHD squeezing flow of different nanofluids over a porous sensor surface in the presence of thermal radiation. Different nanoparticles, including SWCNTs, Al_2O_3, and Cu, and different base fluids, including EO, EG, and water, were considered, and it was observed that the squeezing flow phenomenon greatly depends on the nanoparticle shape. The researchers found that the Al_2O_3/EO, Cu/EG, Cu/EO, and SWCNT/EO nanofluids significantly affect the temperature profile when their concentration, squeeze number, thermal radiation energy, and magnetization parameter are increased.

The effects of nanoparticle shape and size on the hydrothermal behavior of the ZnO, SiO_2, CuO, and Al_2O_3 nanofluids in a horizontal annulus were studied by Bahiraei et al. [149] and Alawi et al. [150]. The comparative results revealed that SiO_2 nanoparticles provided the maximum *Nu* number and pressure drop [150]. They showed that a higher thermal performance can be achieved by applying smaller nanoparticles, and this enhancement was more remarkable at higher fractions. This observation can be attributed to the increased temperature of the nanofluid due to the applied heat flux. Also, smaller particles have more room for collision, and random movement of microscopic particles suspended in the base fluid allows more collisions with molecules of the surrounding medium and reduces the wall temperature. Moreover, it was seen that changing the size of particles does not affect the friction coefficient significantly at low fractions, although this effect becomes important at high fractions. This difference was attributed to the dependency of nanofluid viscosity on the temperature [149]. Furthermore, it was reported that platelet-shaped and cylindrical particles had a higher *Nu* number compared to the other nanoparticle types [150].

Togun et al. [151,152] conducted a comparative 3D numerical and experimental study on the performance of different nanofluids (i.e., TiO_2, CuO, and Al_2O_3) in a concentric annular tube. The setup was an annular pipe with sudden expansion. The heat transfer was enhanced by 49%, 47.3%, and 45.2% for Al_2O_3, CuO, and TiO_2, respectively. The corresponding increases of the pressure drop were 57.6%, 65.4%, and 57.6%. The results showed that the separation regions formed after the sudden expansions considerably affected the heat transfer coefficient, and the separation regions played a significant role in the thermal performance. Moreover, the size of the recirculation zone increased as the *Re* number and expansion ratio increased.

Khan et al. [57] investigated different shapes of the nanoparticles (bricks, cylinders, and platelets) for flow of the nanofluids between parallel plates and indicated that the velocity profile is not a function of the shape of the particles, whereas the temperature profile is significantly affected by the particle shape. Accordingly, the brick-shaped and platelet-shaped particles had the lowest and highest temperature values.

Pena et al. [153] conducted an experimental study on the enhanced thermal behavior of the mineral oil-based nanofluids containing AlN and TiO_2 nanoparticles as a coolant in a vertical annulus. Comparative results revealed that adding TiO_2 nanoparticles was more beneficial compared to adding the AlN nanoparticles.

Although some researchers have examined the effect of nanoparticle shape on nanofluid flow between parallel plates, there is room for many more studies in this area. In reality, rotation of particles is dependent on their shape as well as the type of base liquid. The particle rotation can vary even under magnetic fields, and considering this phenomenon helps to clarify the physical mechanisms behind the nanofluid features in such geometries.

Using hybrid nanofluids is a novel issue in the area of nanofluids. These nanofluids that are produced with the mixing of different kinds of nanoparticles can be utilized in the future as efficient nanofluids for increasing the heat transfer rate. They may present specific attributes when they are used in flows between parallel surfaces. This can open a new subject area for the development of advanced nanofluids with diverse applications.

7. Effect of different dimensionless numbers

In the nondimensional form of governing equations, the impact of various physical processes can be represented by nondimensional numbers or parameters. The exact definition of each nondimensional parameter involves geometrical aspects of the problem and the reference values of parameters. Generally, the Nusselt number denotes the ratio of convective heat transfer to conduction heat transfer, and it is the most important parameter for the study of convective heat transfer. The Reynolds number is a very important parameter for the fluid flow and represents the ratio of inertial fluid to the viscous forces. In boundary layer flows and some forms of nondimensional equations, η is the nondimensional length or similarity variable. The Eckert number represents the strength of heat losses due to friction compared to the enthalpy of the working fluid. The Brownian motion parameter and the thermophoresis parameter denote the strength of the Brownian motion effect and of the thermophoresis effect, respectively. In problems in which the phenomena such as Brownian motion and thermophoresis are important, the ratio of Brownian motion to the thermophoresis can indicate the dominance of each. For example, in the case of thermophoresis being dominant, nanoparticles will tend to be distributed on the basis of the temperature gradient. The Hartmann number is the ratio of Lorentz force to viscous force and indicates the strength of the body force of the magnetic field to the viscous forces.

7.1. Reynolds number, viscosity parameter, and Rayleigh number

In focusing on the forced convection heat transfer and flow characteristics of nanofluids, the effects of the *Re* number and/or the viscosity parameter (R) on the hydrothermal performance of nanofluids are important. These parameters are defined as follows [53,58]:

$$Re = \frac{\rho U_0 h}{\mu_f} \tag{12}$$

$$R = \frac{a h^2}{\nu_f} \tag{13}$$

It should be noted that the viscosity parameter (R) [53] is defined for squeezing flows with the parameter a introduced before.

The influences of the *Re* number and/or the R parameter on the dimensionless velocity profile for nanofluids flowing between parallel plates are analyzed in various studies. Accordingly, it is seen that in the first half of the channel (i.e., $\eta < 0.5$), the velocity along the x-direction tends to decrease with an increase in *Re* or the R parameter; however, an opposite behavior in the velocity is seen for the second half ($0.5 > \eta$), and an accelerated flow is evident [53,57,63,122]. Moreover, the velocity distributions along the y- and z-directions have an inverse relationship with the *Re* and R parameters [50,53,56,57,59,62,63,65,96–98,122]. It is noteworthy that the increase in the *Re* and R parameters leads to the reduction of viscous effects and the decrement of the velocity boundary layer thicknesses.

Furthermore, from the energy transport point of view, it has been revealed that the increment of the *Re* or R parameter reduces the temperature profile of the nanofluid between the two plates. It follows that augmenting the *Re* or R parameter results in a higher *Nu* number and higher skin friction coefficient [53,57,59,63,96–98,122]. Also, researchers have seen the concentration profile increase with the *Re* and R parameters [50,53,65,96–98]. While most of the studies show a direct relationship between the *Re* and R parameters and the *Nu* number, some investigations have reported an opposite relationship. For example, Mahmoudi and Kandelousi [56,62] gave the idea that as *Re* and R parameters increase, the temperature distribution and velocity profile along the y-direction increase slightly and the momentum boundary layer thickness, in turn, is increased. Therefore, the skin friction coefficient and *Nu* number are decreasing functions of the *Re* and R parameters. Interestingly, in another work of Mahmoudi and Kandelousi [61], it is reported that increasing the R parameter results in an enhanced *Nu* number while decreasing the skin friction coefficient.

In annuli, it was evident that for higher *Re* numbers, temperature profiles become steeper. In other words, the effect of nanoparticles on the wall temperature is lessened at higher *Re* numbers. It might be because of the effects of turbulence on the heat transfer. Generally, it has been proven that the heat transfer coefficient varies proportionately with increasing *Re* numbers due to higher fluid velocity [80–86,154]. In addition, as the tube profile becomes an annulus, the contact area between the flow and the tube surface increases; this can increase the friction drag force considerably and consequently lead to an increase in the pressure drop. Moreover, for annular tubes, the flow pattern and velocity distribution will change. This may lead to greater wall shear stresses, resulting in an increment of pressure loss.

To study natural convection heat transfer of nanofluids, the Rayleigh number (*Ra*) is important and is expressed as follows:

$$Ra = \frac{g\beta_f \Delta T L^3}{\alpha_f \nu_f} \tag{14}$$

where g is the gravitational constant, β_f denotes the coefficient of volumetric expansion, L represents the gap between cylinders (r_o–r_i), α_f is the thermal diffusivity, and ν_f is the kinematic viscosity.

Researchers of studies conducted on natural convection heat transfer of nanofluids in concentric annuli have observed that when the *Ra* number is increased, the average *Nu* number is enhanced [138,153,155–160]. The increment of the *Ra* number strengthens the fluid motion, which results in a higher temperature field. Thus, a higher temperature gradient is achieved, thereby enhancing the *Nu* number [156]. Conduction is the dominant mechanism at low Rayleigh numbers ($Ra = 10^3$). However, with increasing *Ra* numbers, the buoyancy forces overcome the viscous forces, and consequently, the convection becomes the dominant mechanism (see Fig. 15). Here, the Rayleigh number shows the strength of the buoyancy effects ($Ra = (g\beta_f \Delta T L^3)/(\alpha_f \nu_f)$), and ψ is the stream function. The subscript of *nf* denotes the nanofluid, and the subscript of max indicates the maximum value. It can be seen from Fig. 15 that the isotherms are uniform at $Ra = 10^3$, whereas they become more distorted at *Ra* numbers of 10^4 and 10^5, indicating the domination of the convection mechanism for the heat transfer. Additionally, the angle of turn for the inner tube boundary condition was found to play a significant role on the streamlines and isotherms, along with the local and average *Nu* numbers [155]. The enhanced *Nu* number values observed at higher Rayleigh numbers indicate the corresponding impact of convection. Meanwhile, a higher enhancement in the heat transfer by the addition of the nanoparticles was reported at relatively lower Rayleigh numbers [155]. This relationship can be attributed to the domination of the conduction mechanism at low Rayleigh numbers, which intensifies the impact of adding high thermal conductive particles to the fluid.

Using the Boussinesq and non-Boussinesq uniform models, Mirzaie and Lakzian [157] conducted a numerical study on the natural convection of a Cu/water nanofluid in a horizontal annulus with discrete source-sink pairs. Different arrangements of the two source-sink pairs were investigated. The sources with constant temperature and sinks were located on the inner and outer cylinders. It was revealed that the increase of the *Ra* number results in an enhancement of the *Nu* number and heat transfer.

Finally, it is noteworthy that heat transfer through natural convection is an essential phenomenon in engineering applications, and

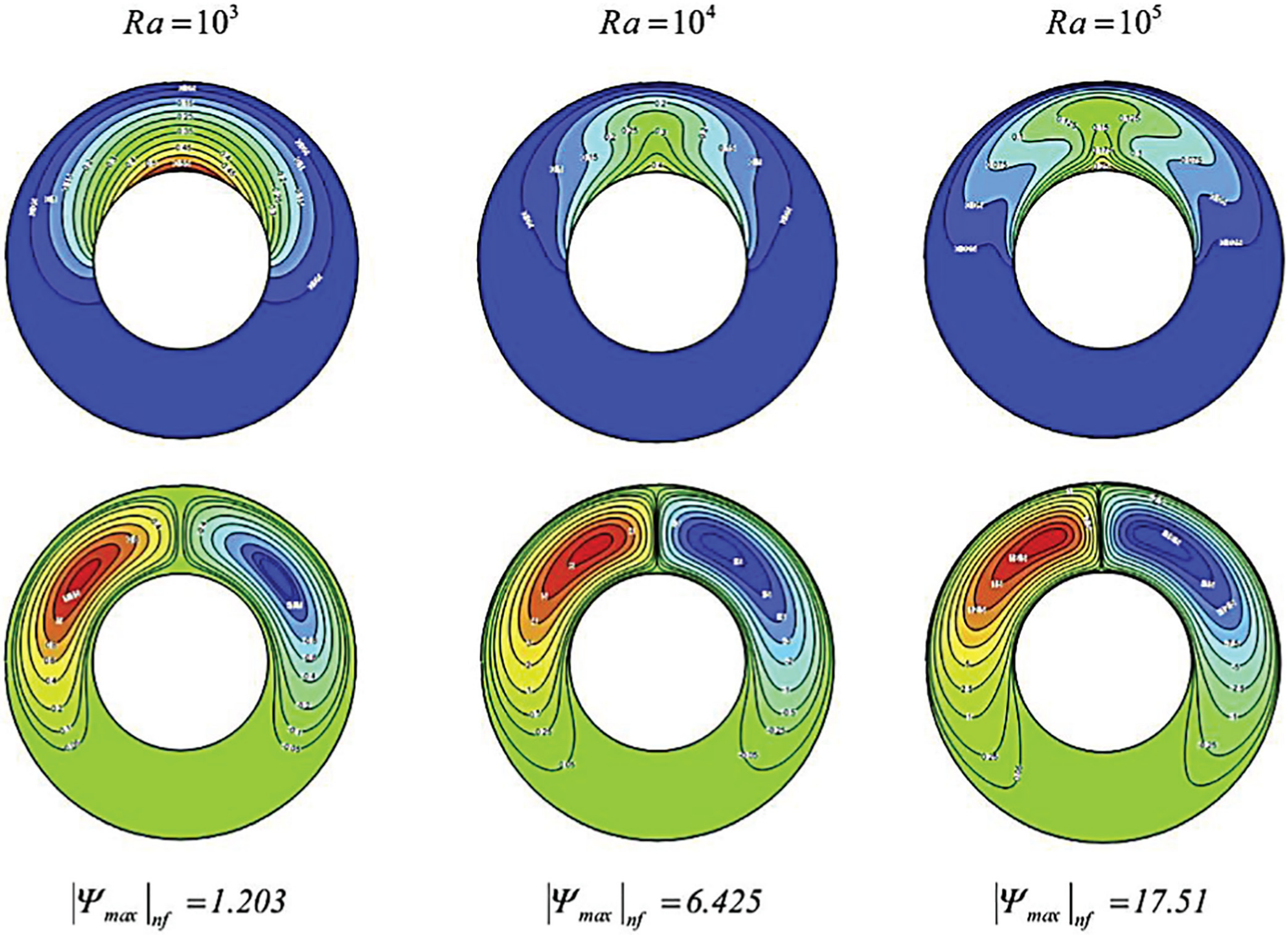

Fig. 15. Comparison of the isotherm (up) and streamline (down) contours for different values of Rayleigh number in a horizontal annulus enclosure: when the top part of the inner cylinder is hot, the volume fraction of nanoparticles is 0.06% and the ratio of diameter of the outer cylinder to the inner cylinder is 2 [155].

therefore, designing optimization approaches for enhancing heat transfer in this field is crucial in the case of using nanofluids. Modeling of the natural convection of nanofluids between parallel plates can be a model for micro-scale devices in which the *Ra* number has a substantial importance.

7.2. Squeeze number

To evaluate the squeezing flow between parallel plates, the squeeze number (S) plays a vital role and is evaluated by Eq. (15) [49]. It should be noted that $S > 0$ and $S < 0$ correspond to the movement of the upper plate away from and toward the lower plate, respectively.

$$S = \frac{\alpha l^2}{2\nu_f} \tag{15}$$

This dimensionless number is related to flows between squeezed parallel plates. To evaluate the impact of squeeze number on the velocity and temperature profiles of the nanofluid between squeezing parallel plates, it should be noted that the negative and positive values of the squeeze number have different impacts on the velocity profile. For the case of squeezing flow ($S < 0$), the axial velocity is increased due to an increment in the squeeze number's absolute value when $\eta < 0.5$, while an inverse trend is observed for $\eta > 0.5$ [68,69,75,76,78]. From a physical point of view, this phenomenon is attributed to the alteration in the fluid velocity. The velocity gradient near the wall region is higher because of the lower fluid velocity in that area. Thus, according to mass conservation law, there should be an increase in the fluid velocity at the central region, which is why at $\eta = 0.5$ a point of separation and backflow occur. By the increase of positive values for the squeeze number, an opposite trend should be observed [68,69,75,76,78].

Since decreasing the squeeze number leads to the increment of the temperature profile and thermal boundary layer thickness, it has been reported that the *Nu* number varies inversely with squeeze number [51,55,66,68–70,72–75,88,133,134]. However, some studies have reported that the *Nu* number varies proportionately with the squeeze number [49,106,130,135,161,162]. The change in the squeeze number can occur due to three factors (see Eq. (15)), namely variation in kinematic viscosity, change of plate distance, and variation in the speed of plate motion. As the plates move apart, the *Nu* number usually decreases; as they come together, though, the *Nu* number is enhanced on account of squeezing flow impact. In fact, the motion of the plates also has a significant effect on nanoparticle migration, which can affect thermal features of nanofluids in these problems. In addition, it has been conceived that the increase of the squeeze number leads to the increment of the skin friction coefficient on both lower and upper surfaces [51,55,70,72,76,88,134,162]. By investigating the effect of the squeeze number on the concentration profile, it was clarified that the increase of the squeeze number increases the nanoparticle concentration profile, and this is the reason for the increase in the skin friction coefficient.

7.3. Eckert number

The Eckert number is defined as per Eq. (16) [106]. Regarding the influence of the Eckert number on the thermal performance of a nanofluid between parallel plates, there is a common conclusion that the temperature profiles increase as the Eckert number increases due to an increase in viscous dissipation. Such a result is also perceived for squeezing flows of nanofluids between parallel plates [67–70,72–76,78,133,134,161,163]. Indeed, a greater Eckert number represents greater drag forces between nanoparticles in the fluid. Thus, heat production is increased, as well as the temperature profile. The Eckert number has a strong effect on the Nu number, and the heat transfer improves with the increase of the Eckert number [51,69,73–75,109,133,161].

$$Ec = \frac{\rho_f}{(\rho c_p)_f}\left(\frac{\alpha x}{2(1-\alpha t)}\right)^2 \quad (16)$$

7.4. Biot and Prandtl numbers

The Biot number (Bi) and Prandtl number (Pr) are two important dimensionless numbers that play important roles in the flow of nanofluids between parallel plates. Notably, the Bi number presents the ratio of the heat transfer resistance inside of a material to that on the material's surface. Moreover, the Pr number shows the ratio of the viscous diffusion rate to the thermal diffusion rate in a fluid. Focusing on the influence of the Bi number and Pr number, Hayat et al. [72] considered the effect of the Bi number on the squeezing flow of water-based SWCNTs and MWCNTs nanofluids and found that the temperature profile varied directly with the Bi number. At higher Bi numbers, a rise in the fluid temperature was observed, which owes to the higher heat transfer rate. The skin friction coefficient was also found to be higher for larger Bi number values [72]. Gupta and Saha Ray [163] and Domairry and Hatami [69] studied the effects of the Prandtl number along with those of the squeeze number, nanoparticle concentration, and the Eckert number on a squeezing unsteady nanofluid flow. The results revealed that the small Pr number values characterize liquid materials that have high thermal diffusivities but low viscosities. The thickness of the thermal boundary layer is reduced at higher Pr numbers. It is apparent that raising the values of the Pr number largely decreases the thermal diffusivity, which decays the thermal boundary layer thickness. Therefore, when the Pr number increases, the temperature field and consequently the local Nu number are rapidly increased.

8. Effect of slip velocity

In problems of small sizes, such as micro/nanoscale sizes, depending on fluid properties and the interfacial roughness, the ‘no-slip boundary condition’ may no longer exist [89]. Thus, it is important to define and consider the slip velocity and slip boundary conditions. In this regard, the slip parameter (λ) is introduced, corresponding to the slip velocity at the surface. Accordingly, higher λ signifies higher slip velocity near walls [89]. The slip velocity on solid surfaces is obtained from the following equation:

$$\lambda = N\frac{\mu_f}{\rho_f}\frac{du}{dr} \quad (17)$$

where N denotes the slip velocity factor.

Ozturk and Kahveci [64] numerically investigated the influences of the slip velocity boundary condition and the Brinkman number (Br) on the flow of nanofluids between parallel plates and reported that the average heat transfer rate decreased with an increase of the Br number. The effect of the slip velocity on the heat transfer decreased when the Br number had lower values. The average heat transfer values got higher with positive values of the Br number, and lower heat transfer values were achieved with negative values of the Br number as the slip velocity increased. Positive values of the Br number mean that the hot wall is heating the fluid, whereas negative values mean that the cold wall is cooling the fluid. Later, Zhu et al. [103] studied the influence of the second-order velocity slip boundary condition [164] and observed that increasing slip velocity was associated with an increase of velocity and a reduction in the temperature.

Focusing on the influence of the slip velocity in squeezing flows of nanofluids, Singh et al. [66] found that the value of the velocity increases near the wall with rising values of the slip velocity when 0 ≤ η ≤ 0.6; for η ≥ 0.6, they found that the velocity decreases as the slip velocity increases. A rise in the values of λ monotonically heightens the fluid temperature. The authors found it evident that the change in the concentration with rising values of λ is negligible. Moreover, they concluded that the increasing value of λ decreases the skin friction coefficient and increases the heat and mass transfer rates. In a squeezing flow, Das et al. [129] considered the effects of the slip velocity and temperature jump along with particle migration and observed that the magnitude of the radial velocity acquires a positive value on the disks' surface in the presence of the slip velocity, which increases with the increase in λ for $\eta < 0.2$ and $\eta > 0.8$. However, for $0.2 \leq \eta \leq 0.8$, the effect is reversed and the fluid velocity decreases with an increase in the values of λ. According to the physics behind this phenomenon, the increased

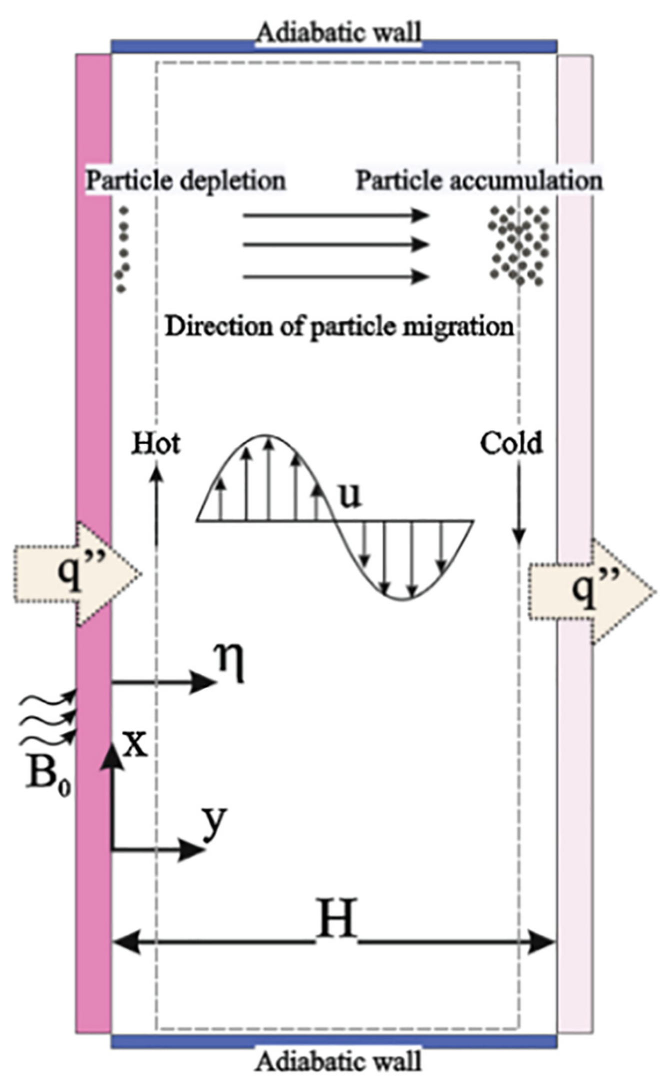

Fig. 16. The description of the physical problem [89].

slip parameter near the wall region decreases the velocity gradient. In addition, increased fluid velocity near the wall will be compensated by a corresponding decrease in the fluid velocity near the central region, as the mass flow rate is kept constant. Moreover, as the slip thermal parameter increases, the temperature of the fluid increases near the lower disk surface, while a reverse behavior occurs near the upper disk surface [129].

Notably, many researchers observed a relative velocity, which is called slip velocity, between the nanoparticles and the base fluid molecules. This observation suggests treating the nanofluid as a two-phase mixture. The main reasons for the slip velocity are temperature rise, the temperature gradient, a rise in volume concentration, the concentration gradient, shear stress, viscosity, and gravity. Due to the slip velocity, the nanoparticles drift or migrate from one region to another [145]. Malvandi et al. [145] reported an increase in the homogeneity of the nanofluid flow (i.e., velocity profile) for higher λ values in an annulus. One can attribute this increase to the increase in the momentum near walls that results in greater heat removal capacity of nanofluids and therefore in eliminating the temperature gradient inside annuli of micro sizes. In another study, Malvandi et al. [165] concluded that higher λ leads to the movement of the momentum in the core region toward the pipe walls and consequently increases the temperature and nanoparticle content at the walls [165]. Thus, the *Nu* number increases at any value of N_{BT} as λ increases. This behavior is more pronounced with lower values of λ. Consequently, the authors found that nanofluids could convey heat more effectively in a slip condition (the nonadherence of fluid to the solid body) than in a no-slip condition. Considering partial velocity slips on the surfaces in the two circular concentric pipes, Turkyilmazoglu [154] evaluated the laminar convective heat transfer of different water-based nanofluids, including the TiO_2, Al_2O_3, CuO, Cu, and Ag nanoparticles within an annulus. It was shown that the velocity slip mechanism played a significant role in the thermal performance, and the velocity slip resulted in anomalous heat transfer improvement, which became even more pronounced with increasing nanoparticle content. Zamani et al. [112] stated that considering the slip condition at the walls improves the heat transportation of conventional fluids more than that of the nanofluids in micro-annular tubes. Also, Malvandi and Ganji [89] revealed that in the presence of a magnetic field, the nanoparticle fraction and temperature profiles are approximately independent of λ, which is a different outcome from that reported in their previous study (i.e., Ref. [165]). Fig. 16 depicts the physical model used in Ref. [89]. The difference between the results of these two studies can be attributed to employing a magnetic field in Ref. [89]. In fact, the transverse magnetic field causes a resistive force termed Lorentz force, which is a delaying force in a descending direction in the vertical annulus.

9. Problems with suction or blowing

The influence of the suction parameter (A) on the hydrothermal analysis of nanofluids between parallel permeable plates is another area that has received attention from researchers. The suction parameter plays a vital role in evaluating problems with suction or blowing and is evaluated in Eq. (18) [135]. In these problems, the suction parameter generally describes two important cases: blowing ($A < 0$) and suction ($A > 0$). In such problems, the lower plate is considered to be a stretching sheet, and the upper one is a solid permeable plate subjected to a constant-flow suction with velocity w_0.

$$A = \frac{w_0}{ah} \tag{18}$$

An investigation of the effect of the *A* parameter on the velocity profiles of a nanofluid revealed that as the *A* parameter increases, the velocity profiles increase [59,62,96]. Furthermore, the thickness of the velocity boundary layer near the lower plate grows, and consequently, the skin friction coefficient decreases with an increase in the *A* parameter [59,62,96,100]. Due to the suction, the fluid existing in more distant regions approaches the surface, which leads to a decrease in the temperature profile because of the reduction in the thickness of the thermal boundary layer. Thus, the *Nu* number increases with the rise of the *A* parameter [59,62,96,99,100]. It is also reported that the concentration increases with the *A* parameter [96]. Rashidi et al. [166] numerically evaluated the MHD flow as well as the heat and mass transfer characteristics of the micro-polar CuO/water and Al_2O_3/water nanofluids between the two parallel porous plates with uniform blowing. They revealed that increasing the blowing velocity causes the radial velocity to increase near the stagnation point but to decrease near the plates. It is interesting that the axial velocity became zero at the stagnation point and increased when the blowing velocity increased far from the plate but not near the stagnation point. Moreover, the temperature and the concentration of the nanofluid decreased with an increase in the blowing velocity in the region between the lower plate and the stagnation point, whereas the behavior was reversed in the region of the stagnation point and the upper plate.

Later, Sheikholeslami and Rokni [99] and Sheikholeslami and Ganji [100] numerically investigated the MHD nanofluid flow as well as the heat and mass transfer between two parallel vertical permeable plates, considering particle migration. They showed that as the *A* parameter increased, the velocity and concentration distributions decreased, but the temperature profile improved. In addition, the influence of the *A* parameter on the skin friction coefficient and on the *Nu* number revealed that the shear stress was a decreasing function and the *Nu* number an increasing function of the *A* parameter. In contrast to in this study, the concentration increased with an increase in the *A* parameter in Ref. [96]. Indeed, in the study of Sheikholeslami and Ganji [100], the plates were vertical, and the effects of particle migration were also considered. The Brownian and thermophoresis impacts were significant in their work, which can be the reason for the alteration in the observed trend of the concentration distribution.

Some researchers have evaluated the effect of the suction parameter for squeezing flows between parallel plates [104–108,110,129,135, 162,167]. The problem configuration is similar to that of Fig. 5 but with permeable disk-shape plate walls. When it comes to the velocity field, it is clear that the velocity decreases for a larger *A* parameter [105,108,135,162]. Indeed, the velocity decreases more quickly in the vicinity of the upper squeezing plate compared with near the lower permeable plate. When the upper surface moves toward the permeable surface, it generates a pressure that accelerates the fluid flow. Therefore, the velocity field at the vicinity of the upper plate increases, thus satisfying the mass conservation principle. The temperature profile, which is dependent on the suction parameter, is another important parameter. The temperature can noticeably change with an increase in the *A* parameter due to the variation of the velocity profile. According to the literature, increasing the *A* parameter decreases the temperature distribution monotonically from $\eta = 0$ to $\eta = 1$ [104,105,108,110]. In fact, the thermal boundary layer becomes thinner at a higher suction parameter due to the higher velocity in this situation, thereby reducing the *Nu* number with an increase in the *A* parameter [104–106,108,162].

This outcome differs from those of most studies conducted on the flow of nanofluids in static parallel plates, which is due to the displacement of the surface in this state. Mohyud-Din et al. [108] numerically investigated the mixed convection heat transfer in the squeezed flow of a nanofluid. They showed that the squeeze number and the skin friction coefficient had a direct relationship for the case of suction and an indirect relationship for the blowing flow. A rise in the skin friction coefficient was observed with an increasing M parameter for the suction flow, and a fall was seen in the blowing case. Moreover, the *Nu* number was a decreasing function of the squeeze number for the case of suction and an increasing function of the squeeze number for the case of blowing. For smaller values of the Brownian motion parameter, the heat transfer rate at the upper disk slightly decreased with an increase in the squeeze number. An opposite behavior was observed for the smaller values of the thermophoresis parameter.

In some of the problems, including suction or blowing related to the flow of nanofluids in parallel plates, the effect of particle migration has been considered. However, it is necessary to apply more complete models involving the influences of the dynamics of particles, entrance impacts, wall-particle interactions, and so on. This can model nanofluids' behavior properly and reduce the contradictions observed in some studies.

10. Presence of a heat source or heat sink

The heat source/sink impacts in convective heat transfer are of noticeable importance where a great temperature difference may occur between the fluid and the surface. The presence of a heat source/sink also occurs in the context of endothermic and exothermic chemical reactions. Heat absorption or generation might vary the temperature distribution in a nanofluid and can influence the particle deposition rate in systems, including nuclear reactors, semiconductors, and electronic devices.

Considering the influence of the presence of a heat source, Rahimi-Gorji et al. [55] and Sheikholeslami and Domiri Ganji [88] simulated the unsteady flow of a squeezed nanofluid under a time-variable magnetic field with the intensity of $B(t) = B_0(1\text{-}\alpha t)$ perpendicular to the plates. They introduced a heat source/sink parameter, which is defined as follows:

$$Hs = \frac{Q_0 l^2}{k_f} \tag{19}$$

It was observed that increasing the heat source parameter leads to a decrease in the temperature profile and a reduction in the temperature boundary layer thickness, and in turn, the *Nu* number is increased.

In the presence of heat generation/absorption, Moshizi and Malvandi [168] analyzed the laminar mixed convective heat transfer of an Al_2O_3/water nanofluid in a vertical annulus. They indicated that a system with heat generation benefitted more from the addition of smaller nanoparticles, whereas the use of larger nanoparticles was suggested for a system with heat absorption. Moreover, Moshizi et al. [169] evaluated two cases, namely heat generation and heat absorption, and found that the enhanced heat transfer coefficient was greater in the former case, especially when the N_{BT} was decreased.

Bouzerzour et al. [170] examined the free convection of a copper-H_2O nanofluid in an annulus. A cool temperature was imposed on the external cylinder, whereas the heaters were located on the internal cylinder. A heat transfer increment was observed via elevating the *Ra* number or the particle content. Placing the heaters on the right and left sides of the internal cylinder produced a greater thermal efficiency.

It should be noted that a heat source or a heat sink might be regarded as invariant, temperature dependent, or space dependent. In most studies performed on the flow of nanofluids in parallel plates, heat sources or heat sinks have been considered to be constant; however, more complete investigations are required that consider a temperature-dependent or space-dependent heat source/sink. For instance, a temperature-dependent heat source can change the temperature distribution and consequently particle migration.

11. Employing non-Newtonian nanofluids

Several studies have reported that adding nanoparticles to Newtonian liquids at relatively high concentrations converts them to non-Newtonian fluids. In other words, nanoparticles can cause a nonlinear relationship between shear stress and strain rate. However, another group of non-Newtonian nanofluids demonstrates non-Newtonian behavior because their base fluids are non-Newtonian. Due to the considerable importance of non-Newtonian nanofluids, some studies have assessed their characteristics between parallel plates. Such investigations were carried out between parallel plates, squeezed channels, and annuli.

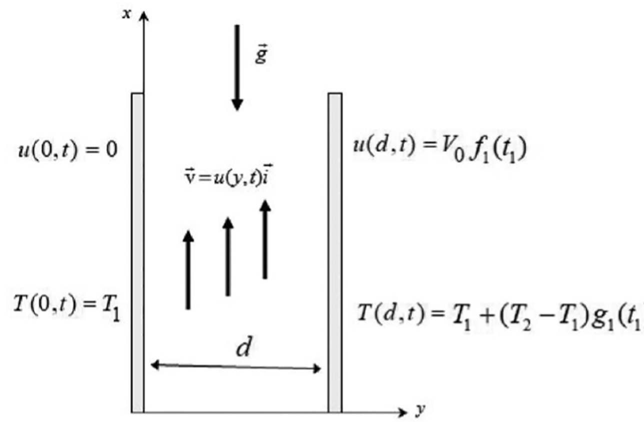

Fig. 17. The physical model used in Ref. [175].

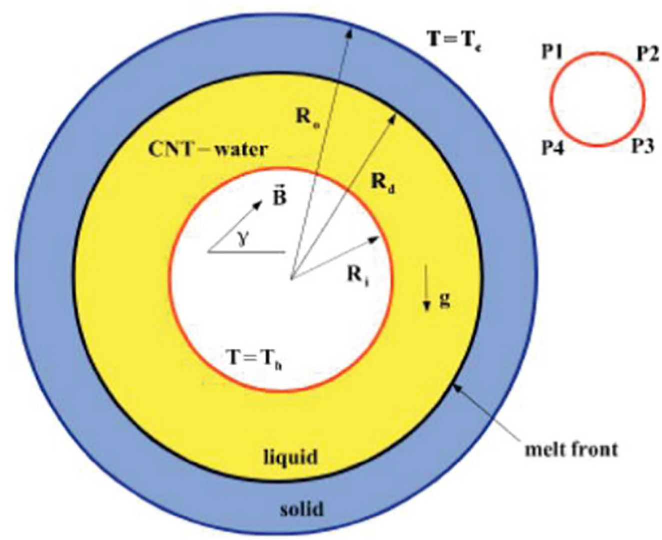

Fig. 18. The schematic of the physical model [176].

Sahebi et al. [171] and Hatami and Ganji [172] numerically studied the flow and natural convection heat transfer of the non-Newtonian nanofluids between two vertical parallel plates. In their work, the base non-Newtonian fluid comprised sodium carboxymethyl cellulose and sodium alginate. It was concluded that increasing the dimensionless non-Newtonian viscosity caused the temperature and velocity values to decrease, but the effect was more significant for the velocity.

Hatami and Jing [67] analyzed an unsteady two-dimensional squeezing flow conveying a non-Newtonian sodium alginate–based nanofluid containing the Cu and Ag nanoparticles between two parallel plates. The authors confirmed that the non-Newtonian viscosity has no impact on the temperature values, but it decreases the velocity profile.

Bahiraei and Alighardashi [173] evaluated the behavior of a non-Newtonian nanofluid consisting of the dispersion of TiO_2 nanoparticles in a mixture of water and 0.5 wt% carboxymethyl cellulose (CMC) in an annulus. As the nanofluid had shear-thinning behavior, increasing the *Re* number decreased the apparent viscosity near walls, which was due to an increased shear rate in these regions. Thus, the velocity profile became flatter, which led to a greater increase in the convective heat transfer coefficient.

The majority of the studies in this context have been conducted on nanofluids with base fluids that have CMC. However, non-Newtonian nanofluids containing carbon-based nanomaterials, such as graphene sheets and carbon nanotubes, are important as well and should be evaluated in the future. Furthermore, the particle migration in non-Newtonian nanofluids may be different from that in Newtonian ones due to the nonlinear relationship between the strain rate and shear stress, which should be considered in future research.

12. Employing advanced nanofluids

Recently some researchers have used advanced nanofluids, including hybrid nanofluids or CNT-based nanofluids, in applications involving flows between parallel plates. Tayebi et al. [174] conducted a numerical simulation using the finite volume method for a Cu-Al_2O_3/water hybrid nanofluid flow in an annulus. They explored the effects of the particle content, the *Ra* number, and the internal heat generation or absorption parameter on the thermohydraulic features and entropy production. The internal heat generation or absorption influenced the heat transfer and entropy generation. The highest flow strength occurred with the largest internal heat production under the conduction-dominated condition. Shah et al. [175] investigated the free convective stream of a bio-nanofluid between two vertical plates (see Fig. 17). A fractional model was employed in the simulation. The responses were stated based on the generalized G-function of Lorenzo, the Hartley function, and the Mittag-Leffler function. For the great time magnitudes, the temperature intensified through the rising of the fractional variable. Moreover, the velocity decreased through the elevation of the fractional variable.

Selimefendigil and Öztop [176] studied the impacts of the combination of a rotational surface and an inclined magnetic field on the mixed convective flow of a CNT-H_2O nanofluid in an annulus (see Fig. 18). They reported that with the rise of the particle content, the mean Nusselt number and the melt fraction increased, whereas an adverse trend occurred for large Hartmann numbers. The heat transfer amount diminished with an increased internal wall rotational speed. The authors argued that the melt front could be controlled with the internal wall's rotation.

Ikram et al. [177] assessed the MHD natural convective stream of a hybrid nanofluid between two parallel plates. They added titanium dioxide and Ag nanoparticles to the water to prepare the hybrid nanofluid. They showed that the *Nu* number enhanced the fractional variable. In addition, the velocity was increased by increasing the Grashof number.

Tayebi et al. [178] performed a numerical study to analyze entropy generation due to free convection inside of an annular channel. The Al_2O_3-copper/H_2O hybrid nanofluid was utilized as the working fluid. For small *Ra* numbers, most entropy production is due to the heat transfer irreversibility, whereas, for large *Ra* numbers, the frictional irreversibility played an important role.

13. Problems including porous media

The impact of porosity is a major area that has received remarkable attention regarding the flow and heat transfer of nanofluids between parallel surfaces. In porous media, the increasing random motion of fluid through the solid matrix leads to an increase in flow mixing and a pressure drop. The former is desirable, and the latter is unfavorable from a hydrothermal viewpoint [179]. Moreover, it is observed that the positive and negative impacts of a nanofluid on heat transfer and a pressure drop, respectively, are more considerable for higher porosities. This is due to the fact that a greater amount of nanofluid exists in a porous medium with high porosity; therefore, the nanofluid has a more pronounced influence on heat transfer enhancement and on an increased pressure drop in a wick structure [180]. Siavashi et al. [179] used a two-phase mixture model as well as a Darcy-Brinkman-Forchheimer relation to simulate an Al_2O_3/water nanofluid flow through an annulus filled with porous media. They showed that special care should be taken in the selection of an appropriate porous medium radius. They observed that for configurations with high permeability ($Da = 0.01$, $Da = 0.1$), the performance efficiency was directly proportional to the porous foam radius, whereas for porous media with medium permeability ($Da = 0.001$), an optimum value was found for the porous medium radius to achieve the greatest efficiency. On the other hand, for a porous foam with further low permeability ($Da = 0.0001$), the efficiency was inversely proportional to the porous foam radius. Furthermore, it was concluded that the employment of porous media with any Darcy number enhances the thermal performance [179]. The Darcy number (Da) denotes the relative influence of the permeability of the medium on a cross-sectional area [179]:

$$Da = \frac{K}{d^2} \tag{20}$$

where K is the permeability of the medium and d represents the characteristic length.

Mashaei et al. [180] analyzed the thermal performance of an Al_2O_3/water nanofluid in an annular porous medium. The results indicated that the thermal performance of the nanofluid was directly proportional to the porosity of the medium and was inversely proportional to its conductivity ratio. Sheremet and Pop [158] studied the influence of porosity on the natural convection of a Cu/water nanofluid in an annulus. The problem considered two media types: glass balls and aluminum foam. They showed that the average *Nu* number was a decreasing function of the porosity of the medium. This is because the heat transfer area

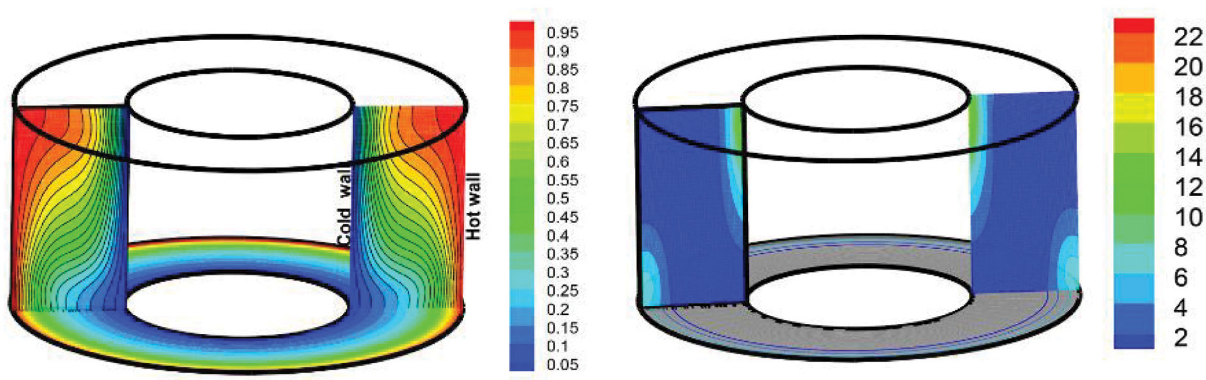

Fig. 19. (a) The temperature distribution and (b) thermal entropy generation for $Ra = 10{,}000$, $Da = 0.1$, and particle concentration of 4% [181].

decreases with an increase in the porosity. Moreover, for the glass balls, the *Nu* number was directly proportional to the nanoparticle content except for in the case of a porosity lower than 0.2, whereas for the aluminum foam, it was inversely proportional to the concentration regardless of the porosity value.

Miles and Bessaïh [181] examined the thermal characteristics and entropy production of a 3D nanofluid flow inside an annulus saturated with a porous medium. The results showed that the Darcy number and the porosity affected the flow pattern, heat transfer, and entropy production. In addition, when the Darcy number and the porosity are increased, the mean Nu number and the Bejan number are enhanced. Fig. 19 illustrates the temperature distribution and entropy generation due to the heat transfer in the annular domain for $Ra = 10{,}000$, $Da = 0.1$, and a particle concentration of 4%.

The majority of published papers in this field (i.e., the flow of nanofluids between parallel surfaces containing porous media) have been carried out in annuli; however, parallel plates containing porous media should also be studied due to their practical utilization in several situations.

14. Effect of considering thermal radiation

For evaluating the effect of thermal radiation on nanofluids' flow and heat transfer, a radiation parameter (*Rd*) is represented as follows [54]:

$$Rd = \frac{4\sigma_e T_c^3}{\beta_R k} \tag{21}$$

Milani Shirvan et al. [54] considered the effect of surface radiation and studied the mixed convection heat transfer of an Al_2O_3/water nanofluid in a solar heat exchanger having parallel surfaces by the mixture model. According to their results, the *Nu* number and pressure drop were directly proportional to the Richardson number and the nanoparticle concentration, and they were indirectly proportional to the nanoparticle diameter and the surface emissivity. In another study, Sheikholeslami et al. [98] studied the influence of thermal radiation on the hydrothermal behavior of nanofluids between parallel plates. The effect of the radiation parameter on the concentration boundary layer thickness was found to be detrimental.

Examining the impact of considering the thermal radiation phenomenon on squeezing flows of nanofluids between parallel plates, Madaki et al. [49], Dogonchi et al. [70], and Sheikholeslami et al. [51] found that an increase in radiation thickens the thermal boundary layer near the upper wall, thereby lowering the *Nu* number there. In another study on the flow of nanofluids between two parallel plates, Sheikholeslami and Ganji [161] considered thermal radiation and particle migration in their analysis. They observed that as the *Rd* parameter increases, the temperature boundary layer becomes thinner, and the concentration profile is increased. Thus, the *Nu* number is an increasing function of the *Rd* parameter. Moreover, Hayat et al. [130] studied the unsteady squeezed flow past a Riga plate under a magnetic field. A Riga plate is a span-wise adjusted cluster of alternating electrodes and changeless magnets mounted on a plane surface, which is known as the electromagnetic actuator. According to their results, a higher temperature and an enhanced *Nu* number were observed for a larger *Rd* parameter.

Sheikholeslami et al. [136] studied the nanofluid flow between two circular cylinders in a magnetic field and considered the effect of thermal radiation. They reported that the temperature gradient decreased with an increase in the *Rd* parameter.

Frequently, the reported results show that the *Nu* number is enhanced with an increase of the *Rd* parameter. In fact, an increase in the *Rd* parameter results in a temperature increase in nanofluids, and the change is more gradual compared with lower *Rd* values. This can also influence the mechanisms of particle motion, such as Brownian motion and thermophoresis.

15. Effects of rotation

Many researchers evaluated the characteristics of nanofluid flowing between two parallel surfaces when the plates and the fluid rotate together with angular velocity Ω around an axis that is perpendicular to the plates' surface. The rotation parameter (*Kr*) plays a vital role in evaluating the problems considering the rotating system and is evaluated in Eq. (22) [50].

$$Kr = \frac{\Omega h^2}{v_f} \tag{22}$$

Investigations into the velocity variation of nanofluids' flow between parallel plates reveal that as the *Kr* parameter increases, the Coriolis force is increased, leading to an increase in the rotational velocity [96–98,101]. For the growing value of the *Kr* parameter, the transverse velocity profile increases from $\eta = 0$ to 0.2 and begins to decrease afterward, whereas the velocity distribution in the *y* direction monotonically decreases for higher values of the *Kr* parameter [50,59,63,65,96–98,122]. These studies show that the Coriolis force has an inverse impact on the transverse velocity in the *z* direction compared with the Lorenz force, meaning that the transverse velocity decreases with a higher *Kr* parameter. Furthermore, it is found that the thickness of the temperature boundary layer decreases with an increase in the Coriolis force, and as the *Kr* parameter is increased, the skin friction coefficient is increased while the *Nu* number is reduced [59,63]. According to Mahmoodi and Kandelousi [56], as the *Kr* parameter increases, the Coriolis force is increased, thus resulting in a thicker thermal boundary layer, and as a result, a higher *Nu* number will be obtained. In addition, it was observed that the skin friction coefficient decreased as a function of the *R* and *Kr* parameters.

El-Maghlany et al. [182] conducted an experimental investigation of the thermal behavior of a horizontal double-tube counter-flow heat exchanger with a rotating inner tube. The effectiveness and the number of transfer units (NTU) increased by about 16.5% and 23.4%, respectively, and the pressure drop increased by about 36% through the addition of 3 vol% Cu nanoparticles into the base fluid. It was observed that the rotation of the inner tube significantly increased the NTU with pressure drop penalties. The effectiveness and the NTU increased by about 30.7% and 51.4%, and the pressure drop increased by 136% for3 vol% and a rotation of 500 rpm. The authors concluded that adding the nanoparticles is highly beneficial and is more preferred rather than rotating the inner tube. In another study, Malvandi and Ganji [183] theoretically

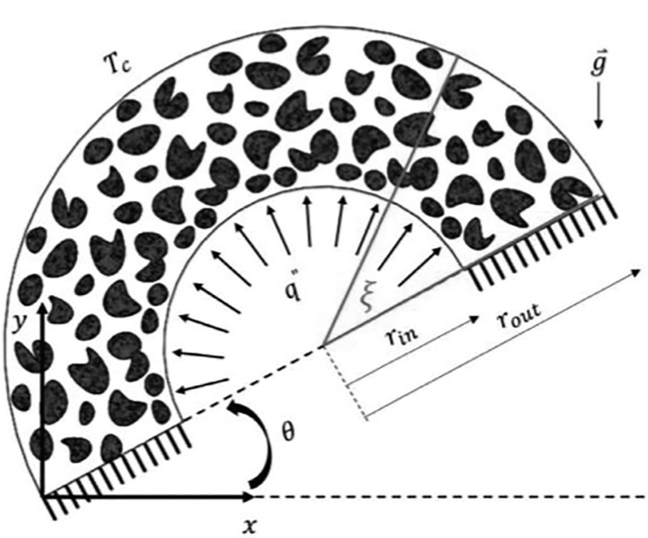

Fig. 20. Schematic of the half-annulus cavity having the porous material [184].

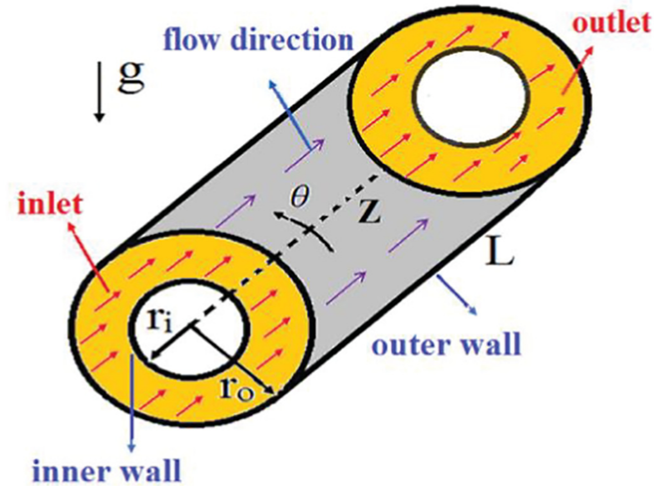

Fig. 21. The annulus under investigation [186].

studied the convective heat transfer of an Al_2O_3/water nanofluid inside of a horizontal annulus in which the inner tube had a streamwise movement. Two cases were studied: (I) the inner tube was under a constant heat flux, and the outer tube had an adiabatic condition, and (II) the outer tube was under a constant heat flux, and an adiabatic boundary condition for the inner tube was considered. The movement of the inner cylinder was found to be beneficial in Case II and detrimental in Case I.

Because the rotation of the surfaces changes the temperature and the velocity profiles of nanofluids, it can influence entropy generation and irreversibility rates. Indeed, it is known that temperature and velocity distributions affect entropy generation. As a result, analyses in this area, with the aid of the second law of thermodynamics, are strongly needed in future investigations.

16. Using advanced methods

For analyzing nanofluid flows between parallel plates and in annuli, some investigators have used more advanced methods, including the two-phase flow analysis. Yekani Motlagh et al. [184] studied the natural convective flow of a nanofluid in a porous semi-annulus cavity via a two-phase flow model. The enclosure was filled with a Fe_3O_4–H_2O nanofluid (see Fig. 20). Due to the thermophoresis effects, the particle distribution near the outside cylinder with a constant temperature boundary condition was greater than that in the case of the constant flux for the inner cylinder. Also, the particle distribution was more uniform for the larger porous *Ra* numbers.

Siavashi and Rostami [185] researched the free convective heat transfer and entropy production of an Al_2O_3 nanofluid in a cylindrical annular enclosure. The cavity possessed a concentric circular heat source, which was covered with a permeable material. The nanofluid was simulated using the two-phase mixture approach. The results showed that the shear-thinning nanofluid led to a greater Nusselt number compared with the other ones. Moreover, the lowest entropy production level and the greatest performance coefficient were observed for the fully porous enclosure. Rezaei Gorjaei et al. [186] employed the two-phase mixture method to simulate the flow of a water-alumina nanofluid within a 3D concentric annulus. As shown in Fig. 21, the enclosure's surfaces were subjected to the constant temperature boundary condition. It was revealed that the bottom of the annulus and the upper side of the internal wall had larger particle content. Furthermore, the heat transfer and the thermal entropy production intensified with an increase in the particle content and the *Re* number. In addition, the smallest and greatest levels of thermal entropy production occurred in the annulus's core section and in the vicinity of the surfaces, respectively.

Other researchers used the Lattice Boltzmann method (LBM) in their studies of the flow of nanofluids between parallel plates and within annuli. Jourabian et al. [187] used an enthalpy-based LBM to simulate a phase change material (PCM) melting inside an elliptical annulus. The results unveiled that the annulus inclination had no significant effect on the liquid fraction. Adding the nanoparticles was introduced as the best method for enhancing the liquid fraction. Using the porous material was also suggested in the inclined and prolate structures. Ashraf et al. [188] studied the nanofluid stream and the heat transfer within an annulus via the multi-relaxation-time LBM. When the particle content and the *Ra* number increased from the minimum magnitude to the maximum magnitude, the largest improvements in the mean *Nu* number were approximately 45% and 94%, respectively. Moreover, the greatest intensification in the overall entropy production was about 57%, with an increase in the *Ra* number.

Usman et al. [189] modified the Legendre wavelets method (LWM) to investigate the unsteady stream of a nanofluid between two parallel plates. The parameters of the squeeze and permeable velocity reduced the friction, whereas a reverse trend was perceived for the Hartmann number. The authors claimed that the suggested modification is efficient and can be developed for other nonlinear situations.

17. Effects of heat flux ratio, radius ratio, and inclination angle in annuli

The heat flux ratio ($\varepsilon = q_i''/q_o''$), radius ratio ($\zeta = r_i/r_o$), and inclination angle are three important parameters affecting the hydrothermal characteristics of nanofluids in annuli. Contrary to the circular tubes, in which the heat transfer coefficient is independent of the heat flux, the heat transfer coefficient of annuli is significantly dependent on the heat flux ratio [149]. The nanofluid near the inner wall becomes locally concentrated for $\varepsilon < 1$, resulting in a reduced local heat transfer. The nanoparticle content peak shifts toward the outer wall by increasing ε to more than 1. However, when $\varepsilon < 1$, the local concentrated region of nanoparticles moves toward the inner wall due to a higher temperature gradient near the outer wall and consequently a higher particle migration toward the inner wall. However, when ε becomes zero, nanoparticles accumulate at the inner wall because no temperature gradient exists at the inner wall for $\varepsilon = 0$ [109,138]. Overall, all of these trends can be attributed to the significant impact of thermophoresis on particle migration, which affects temperature gradients as well.

The temperature and velocity profiles of nanofluids are also a significant function of the distribution of nanoparticles and thus of ε [111]. It is reported that the velocity profile becomes nonuniform, and its peak moves toward the wall with a higher heat flux [144]. On the other hand, an opposite variation is observed for the temperature profile versus the heat flux. In fact, the dip point in the temperature profile tends to move toward the wall with a lower heat flux. Therefore, in a configuration with two heat fluxes, such as micro-annuli, different modes of particle migration appear. It should be mentioned that with an increase in the heat flux on a wall, the Brownian motion and thermophoresis on the wall intensify and should be considered when one is modeling for problems involving the heat flux ratio; however, slight efforts have been made regarding this issue.

Although nanofluids provide a higher heat transfer rate, base fluids are preferred in terms of the figure of merit (FoM). It is reported that nanofluids have a lower FoM compared with base fluids. The lower value of the FoM is attributed to an increase in the pressure drop through the addition of nanoparticles [111]. In this regard, the use of smaller nanoparticles is recommended because they can significantly improve thermal efficiency while not significantly affecting the pressure drop. When $\varepsilon > 1$, the use of nanoparticles is found to be inefficient in terms of the FoM, whereas when $\varepsilon < 1$, some conditions are obtained that provide a remarkable increase in thermal efficiency and the FoM.

Various studies have also been conducted to investigate the effect of the radius ratio or aspect ratio on the hydrothermal performance of nanofluids in annuli. It was found that the radius ratio can significantly affect the heat transfer rate in annuli. For instance, when $\varepsilon = 0.4$ and $\zeta = 0.6$, a 60% improvement in the thermal performance of nanofluids is reported in Ref. [111]. Accordingly, one can find that tuning the radius ratio, especially at lower heat flux ratios, can significantly enhance nanofluids' thermal performance. It is found that the higher ζ leads to shifting the velocity profile toward the inner wall due to strengthening the impact of viscous forces [111,137,144]. Consequently, a lower temperature gradient is reported for nanofluids as ζ increases. In fact, a higher ζ corresponds to a higher surface area available for heat transfer, which results in an improvement in the amount of heat adsorption at the inner wall. Accordingly, the particle migration near the inner wall will increase, which causes a diluted region and, in turn, a higher velocity near the inner wall as ζ increases [145].

When $\varepsilon < 1$, the sensitivity of the heat transfer rate to ζ is significant, especially for a lower ζ [111]. For this condition (i.e., lower ζ and ε), the direction of heat transfer changes at the inner wall due to the superiority of the surface area and the corresponding heat flux at the outer wall compared to at the inner wall [144]. Keeping ε constant while increasing ζ results in higher heat transfer rates up to an optimum rate, after which the heat transfer decreases due to the significant impact of viscous forces. Accordingly, an optimum range exists for ζ when $\varepsilon < 1$, which leads to the highest thermal performance [111,137,144]. For instance, Malvandi et al. [145] and Moshizi and Pop [142] presented optimum ζ values of 0.5 and 0.3, respectively, where the heat transfer peaks. However, an ascending trend is observed for the heat transfer with ε and ζ when $\varepsilon > 1$ [111,137,144]. Moreover, apart from nanofluids' thermal performance, its pressure drop is found to slightly decrease at a higher ζ except for with higher values of ε [111,137,144].

Zamani et al. [112] employed a modified Buongiorno model [113] to numerically investigate the thermal performance of the Al_2O_3/water nanofluids in a horizontal concentric annulus. They considered the heterogeneous nanofluid flow under two boundary conditions: Case (I) the outer tube had a constant temperature, and the inner one was adiabatic, and Case (II) the outer tube was isolated, and the inner one had a constant temperature. It was shown that in Case II, with an increase in ζ, more heat was absorbed in the inner wall, which led to the accumulation of nanoparticles at the adiabatic outer wall. Meanwhile, in Case I, the nanoparticle content decreased at the adiabatic inner wall. Moreover, increasing the radius ratio for Case I led to a rise in the pressure drop increase as well as a reduction in the heat transfer enhancement. An opposite trend was seen for Case II. Therefore, it was concluded that Case I is more beneficial when the ratio of inner to outer radii has smaller values, whereas Case II is proper for larger ratios [112].

Siavashi and Jamali [190] found that the *Nu* number changes slightly with the use of different ζ values for a nanofluid turbulent flow, which was in contrast to the laminar flow inside of an annulus where the radius ratio has a more profound influence on the *Nu* number [191]. This phenomenon was reported to be independent of the nanoparticle content, and the same behavior can be observed at different φ values. In general, several researchers proposed that the heat transfer rate of nanofluids in annuli is a decreasing function of ζ [155,158,160,190,192], whereas some others illustrated a direct relationship of the *Nu* number and ζ [136,143,150]. For instance, Fallah et al. [156] employed LBM to investigate the laminar natural convection of the Al_2O_3/water nanofluids in a horizontal annulus enclosure. It was

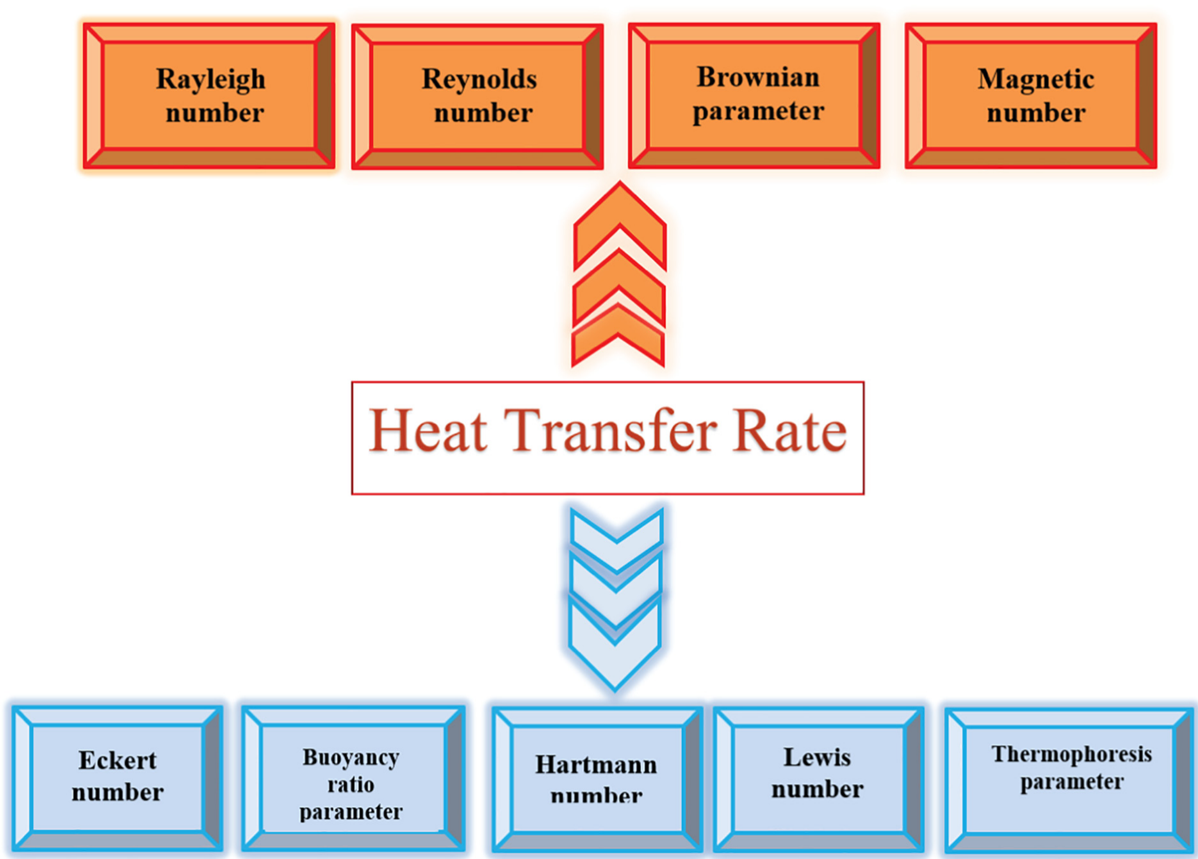

Fig. 22. Summary of the general effects of the analyzed non-dimensional numbers and parameters on the rate of heat transfer in the space between two plates.

reported that at a constant *Ra* number, the *Nu* number was inversely proportional to the annulus gap width ratio $(2R_i/(R_o-R_i))$.

It is noteworthy that the *Nu* number in these papers means the average *Nu* number on both walls of the annulus. In reality, the *Nu* number may increase on a wall and decrease on another wall when the radius ratio changes.

Some studies dealt with inclined annuli. In fact, the inclination angle can have noticeable effects on the flow patterns of nanofluids in these geometries. Imani et al. [193] showed that the inclination angle significantly altered the *Nu* number at the inner tube and had a weaker impact on the *Nu* number at the outer tube. The negative angles led to a greater enhancement in the *Nu* number compared with the positive angles. On the other hand, the local friction factor was found to be greater at positive angles. In another study, Izadi et al. [194] showed that in an inclined annulus, the flow regime was a significant function of secondary flows as well as the axial component of buoyancy forces. Therefore, the highest thermal performance was observed in the horizontal condition due to the greatest secondary flow and buoyancy forces in this condition. When the inclination angle is increased (clockwise or counterclockwise), the effect of the buoyancy-induced secondary flow decreases, and the buoyancy accelerating force increases due to the gravity force direction.

18. Concluding remarks and future directions for research

The flow between parallel surfaces has many applications in thermal systems. Also, it has been established that nanofluids as new working fluids have the potential to enhance thermal systems' performance. The present review article dealt with the flow between parallel surfaces where a nanofluid is the working fluid. Researchers in the majority of works considered the forced convection laminar flow of nanofluids through horizontal parallel surfaces and used a single-phase simulation for evaluating the working fluids. The impacts of various important influential parameters, including Brownian motion and thermophoresis, and viscous dissipation are well understood and described. Furthermore, various investigations examined the effects of rotation, radiation, porosity, the presence of heat sources, and boundary conditions, such as slip velocity, temperature jump, and suction/blowing.

A summary of the general effects of the analyzed non-dimensional numbers and parameters on the rate of heat transfer in the space between two plates is provided in Fig. 22. The effects of most of these parameters are almost independent of the thermal boundary conditions. The impact of raising these parameters and numbers on the heat transfer rate is graphically depicted. Here, the Reynolds number and the Rayleigh number indicate the strength of the fluid motion. Increasing these two numbers always enhances the heat transfer. The Brownian motion parameter, thermophoresis parameter, the buoyancy ratio parameter, and Lewis number are related to the nanoparticles. Among these parameters, only the Brownian motion parameter tends to enhance the heat transfer, and the remaining parameters tend to decrease the heat transfer. The magnetization parameter and the Hartmann number are related to the ferrohydrodynamic and MHD flows, respectively. The magnetization parameter tends to enhance the heat transfer, whereas the Hartmann number tends to decrease the heat transfer. The viscous dissipation effect in the form of the Eckert number tends to reduce the heat transfer.

Accordingly, the lack of numerical investigations concerning the turbulent nanofluid flow and heat transfer between the parallel surfaces is a significant gap and indicates a direction for future work. Moreover, studies focusing on nanofluid exergy efficiency and entropy generation are scarce. A few investigations have focused on the natural and mixed convection of nanofluids in vertical geometries. The nanoparticle composition, shape, and size are other parameters that have not been well considered. Therefore, further research efforts are needed to elucidate the thermal behavior of nanofluids in such cases.

Regarding the behavior of nanofluids under a magnetic field, the present review showed that a simplified form of the magnetic field has been used in numerical studies. However, practical magnetic fields, such as those created by a current-carrying wire or a field around permanent magnets, are 3D magnetic fields with complex patterns, which should be examined in future studies.

It was understood that the commonly used mathematic model is the single-phase (homogeneous) approach. In the homogeneous model, the nanoparticles are scattered uniformly, and it highly depends on models of the effective properties, which is an unrealistic approach. When two-phase models are employed, some factors, such as dispersion, sedimentation, the Brownian diffusion, and the friction between nanoparticles and the carrier fluid, are also included in the model and will result in more realistic results. However, with respect to the limitations of the computational tools, this approach is limited to a volume containing finite particles. Therefore, it is suggested that alternative approaches, such as the LBM, can be employed to yield reliable results and determine the features of nanofluids. Although the LBM can properly simulate energy transportation in nanofluids' flow without particle limitations, very few investigations have adopted this method in the field of the mixed and forced convection of nanofluids.

Overall, the use of nanofluids is found to be very promising for a variety of purposes. However, their use in industry is limited for various reasons, including the inconsistency of the results of various works. It may be due to a poor theoretical understanding of the corresponding mechanisms or the poor characterization of the suspensions. Accordingly, further research is needed to address this lack of information and foster a better understanding of nanofluids. The future studies could address the following questions:

(I) What are the key energy transport mechanisms?
(II) What are the main parameters affecting the thermal conductivity of nanofluids, such as particle shape and particle agglomeration?
(III) What is the impact of surfactant molecules on the physical properties and on system performance? This is of importance because acquiring high-quantity nanofluids with high temperatures and prominent long-term stability for various applications is necessary for most industrial applications.
(IV) How does a pressure drop or the pumping power affect the performance of nanofluids for engineering purposes? The increase in the thermal performance of fluids through the addition of nanoparticles is always associated with an increase in the pressure drop. Therefore, information about the pumping power loss is insightful.

Declaration of Competing Interest

None

References

[1] Mahian O, Bellos E, Markides CN, Taylor RA, Alagumalai A, Yang L, et al. Recent advances in using nanofluids in renewable energy systems and the environmental implications of their uptake. Nano Energy. 2021;86:1–28 106069.
[2] Hemmat Esfe M, et al. Application of conventional and hybrid nanofluids in different machining processes: a critical review. Adv Colloid Interface Sci. 2020;282:102199.
[3] Amani M, Amani P, Jumpholkul C, Mahian O, Wongwises S. Hydrothermal optimization of SiO 2/water nanofluids based on attitudes in decision making. Int Commun Heat Mass Transf. 2018;90:67–72.
[4] Nikolov A, Wu P, Wasan D. Structure and stability of nanofluid films wetting solids: an overview. Adv Colloid Interface Sci. 2019;264:1–10.
[5] Amani M, Amani P, Mahian O, Estellé P. Multi-objective optimization of thermophysical properties of eco-friendly organic nanofluids. J Clean Prod. 2017;166:350–9. https://doi.org/10.1016/j.jclepro.2017.08.014.
[6] Lu G, Wang XD, Duan YY. A critical review of dynamic wetting by complex fluids: from Newtonian fluids to non-Newtonian fluids and nanofluids. Adv Colloid Interface Sci. 2016;236:43–62.
[7] Ganvir RB, Walke PV, Kriplani VM. Heat transfer characteristics in nanofluid—A review. Renew Sustain Energy Rev. 2017;75:451–60.

[8] Solangi KKHK, Kazi SSN, Luhur MMR, Badarudin A, Amiri A, Sadri R, et al. A comprehensive review of thermo-physical properties and convective heat transfer to nanofluids. Energy. 2015;89:1065–86.
[9] Suganthi KS, Rajan KS. Metal oxide nanofluids: review of formulation, thermo-physical properties, mechanisms, and heat transfer performance. Renew Sustain Energy Rev. 2017;76:226–55.
[10] Lomascolo M, Colangelo G, Milanese M, de Risi A. Review of heat transfer in nanofluids: conductive, convective and radiative experimental results. Renew Sustain Energy Rev. 2015;43:1182–98.
[11] Hussein AM, Sharma KV, Bakar RA, Kadirgama K. A review of forced convection heat transfer enhancement and hydrodynamic characteristics of a nanofluid. Renew Sustain Energy Rev. 2014;29:734–43.
[12] Haddad Z, Oztop HF, Abu-Nada E, Mataoui A. A review on natural convective heat transfer of nanofluids. Renew Sustain Energy Rev. 2012;16:5363–78.
[13] Pinto RV, Fiorelli FAS. Review of the mechanisms responsible for heat transfer enhancement using nanofluids. Appl Therm Eng. 2016;108:720–39.
[14] Mahian O, Kolsi L, Amani M, Estellé P, Ahmadi G, Kleinstreuer C, et al. Recent advances in modeling and simulation of nanofluid flows-part I: fundamental and theory. Phys Rep. 2018. https://doi.org/10.1016/j.physrep.2018.11.004.
[15] Mahian O, Kolsi L, Amani M, Estellé P, Ahmadi G, Kleinstreuer C, et al. Recent advances in modeling and simulation of nanofluid flows-part II: applications. Phys Rep. 2018. https://doi.org/10.1016/j.physrep.2018.11.003.
[16] Vanaki SM, Ganesan P, Mohammed HA. Numerical study of convective heat transfer of nanofluids: a review. Renew Sustain Energy Rev. 2016;54:1212–39.
[17] Sheikholeslami M, Ganji DD. Nanofluid convective heat transfer using semi analytical and numerical approaches: a review. J Taiwan Inst Chem Eng. 2016;65:43–77.
[18] Bahiraei M. A comprehensive review on different numerical approaches for simulation in Nanofluids: traditional and novel techniques. J Dispers Sci Technol. 2014;35:984–96.
[19] Zhao N, Guo L, Qi C, Chen T, Cui X. Experimental study on thermo-hydraulic performance of nanofluids in CPU heat sink with rectangular grooves and cylindrical bugles based on exergy efficiency. Energ Conver Manage. 2019;181:235–46.
[20] Qi C, Tang J, Fan F, Yan Y. Effects of magnetic field on thermo-hydraulic behaviors of magnetic nanofluids in CPU cooling system. Appl Therm Eng. 2020;179:115717.
[21] Zhao N, Qi C, Chen T, Tang J, Cui X. Experimental study on influences of cylindrical grooves on thermal efficiency, exergy efficiency and entropy generation of CPU cooled by nanofluids. Int J Heat Mass Transf. 2019;135:16–32.
[22] Fan F, Qi C, Tang J, Liu Q, Wang X, Yan Y. A novel thermal efficiency analysis on the thermo-hydraulic performance of nanofluids in an improved heat exchange system under adjustable magnetic field. Appl Therm Eng. 2020;179:115688.
[23] Qi C, Luo T, Liu M, Fan F, Yan Y. Experimental study on the flow and heat transfer characteristics of nanofluids in double-tube heat exchangers based on thermal efficiency assessment. Energ Conver Manage. 2019;197:111877.
[24] Younes H, Christensen G, Li D, Hong H, Al Ghaferi A. Thermal conductivity of nanofluids: review. J Nanofluids. 2015;4:107–32.
[25] Tawfik MM. Experimental studies of nanofluid thermal conductivity enhancement and applications: a review. Renew Sustain Energy Rev. 2017;75:1239–53.
[26] Aybar HŞ, Sharifpur M, Azizian MR, Mehrabi M, Meyer JP. A review of thermal conductivity models for nanofluids. Heat Transf Eng. 2015;36:1085–110.
[27] Murshed SMS, Estellé P. A state of the art review on viscosity of nanofluids. Renew Sustain Energy Rev. 2017;76:1134–52.
[28] Bashirnezhad K, Bazri S, Safaei MR, Goodarzi M, Dahari M, Mahian O, et al. Viscosity of nanofluids: a review of recent experimental studies. Int Commun Heat Mass Transf. 2016;73:114–23.
[29] Meyer JP, Adio SA, Sharifpur M, Nwosu PN. The viscosity of nanofluids: a review of the theoretical, empirical, and numerical models. Heat Transf Eng. 2016;37:387–421.
[30] Azmi WH, Sharma KV, Mamat R, Najafi G, Mohamad MS. The enhancement of effective thermal conductivity and effective dynamic viscosity of nanofluids – a review. Renew Sustain Energy Rev. 2016;53:1046–58.
[31] Kasaeian A, Azarian RD, Mahian O, Kolsi L, Chamkha AJ, Wongwises S, et al. Nanofluid flow and heat transfer in porous media: a review of the latest developments. Int J Heat Mass Transf. 2017;107:778–91.
[32] Mahian O, Kianifar A, Kalogirou SA, Pop I, Wongwises S. A review of the applications of nanofluids in solar energy. Int J Heat Mass Transf. 2013;57:582–94.
[33] Kasaeian A, Eshghi AT, Sameti M. A review on the applications of nanofluids in solar energy systems. Renew Sustain Energy Rev. 2015;43:584–98.
[34] Bahiraei M, Rahmani R, Yaghoobi A, Khodabandeh E, Mashayekhi R, Amani M. Recent research contributions concerning use of nanofluids in heat exchangers: a critical review. Appl Therm Eng. 2018. https://doi.org/10.1016/j.applthermaleng.2018.01.041.
[35] Bahiraei M, Hangi M. Flow and heat transfer characteristics of magnetic nanofluids: a review. J Magn Magn Mater. 2015;374:125–38.
[36] M'hamed B, Sidik NAC, Yazid MNAWM, Mamat R, Najafi G, Kefayati GHR. A review on why researchers apply external magnetic field on nanofluids. Int Commun Heat Mass Transf. 2016;78:60–7.
[37] Amani P, Amani M, Ahmadi G, Mahian O, Wongwises S. A critical review on the use of nanoparticles in liquid–liquid extraction. Chem Eng Sci. 2018;183. https://doi.org/10.1016/j.ces.2018.03.001.
[38] Togun H, Abdulrazzaq T, Kazi SN, Badarudin A, Kadhum AAH, Sadeghinezhad E. A review of studies on forced, natural and mixed heat transfer to fluid and nanofluid flow in an annular passage. Renew Sustain Energy Rev. 2014;39:835–56.
[39] Dawood HK, Mohammed HA, Che Sidik NA, Munisamy KM, Wahid MA. Forced, natural and mixed-convection heat transfer and fluid flow in annulus: a review. Int Commun Heat Mass Transf. 2015;62:45–57.
[40] Kakac S, Pramuanjaroenkij A, Kakaç S, Pramuanjaroenkij A. Review of convective heat transfer enhancement with nanofluids. Int J Heat Mass Transf. 2009;52:3187–96.
[41] Hussain A, Mohyud-Din ST, Cheema TA. Analytical and numerical approaches to squeezing flow and heat transfer between two parallel disks with velocity slip and temperature jump. Chinese Phys Lett. 2012;29:114705.
[42] Ahmed HE, Ahmed MI. Thermal performance of annulus with its applications; a review. Renew Sustain Energy Rev. 2017;71:170–90.
[43] Fischer P, Windhab EJ. Rheology of food materials. Curr Opin Colloid Interface Sci. 2011;16:36–40. https://doi.org/10.1016/j.cocis.2010.07.003.
[44] Lim AS, Lopatnikov SL, Wagner NJ, Gillespie JW. Investigating the transient response of a shear thickening fluid using the split Hopkinson pressure bar technique. Rheol Acta. 2010;49:879–90. https://doi.org/10.1007/s00397-010-0463-8.
[45] Lin J-R. Non-Newtonian squeeze film characteristics between parallel annular disks: Rabinowitsch fluid model. Tribol Int. 2012;52:190–4. https://doi.org/10.1016/j.triboint.2012.02.017.
[46] Rowland HD, King WP, Pethica JB, Cross GLW. Molecular confinement accelerates deformation of entangled polymers during squeeze flow. Science. 2008;80(322):720–4. https://doi.org/10.1126/science.1157945.
[47] Sukumaran K, Ravikumar KK, Pillai SGK, Rajan TPD, Ravi M, Pillai RM, et al. Studies on squeeze casting of Al 2124 alloy and 2124-10% SiCp metal matrix composite. Mater Sci Eng A. 2008;490:235–41. https://doi.org/10.1016/j.msea.2008.01.054.
[48] Farjoud A, Cavey R, Ahmadian M, Craft M. Magneto-rheological fluid behavior in squeeze mode. Smart Mater Struct. 2009;18:095001. https://doi.org/10.1088/0964-1726/18/9/095001.
[49] Madaki AG, Roslan R, Rusiman MS, Raju CSK. Analytical and numerical solutions of squeezing unsteady Cu and TiO 2 -nanofluid flow in the presence of thermal radiation and heat generation/absorption. Alex Eng J. 2017. https://doi.org/10.1016/j.aej.2017.02.011.
[50] Hatami M, Mosayebidorcheh S, Jing D. Two-phase nanofluid condensation and heat transfer modeling using least square method (LSM) for industrial applications. Heat Mass Transf. 2017. https://doi.org/10.1007/s00231-016-1964-5.
[51] Sheikholeslami M, Ganji DDD, Rashidi MMM. Magnetic field effect on unsteady nanofluid flow and heat transfer using Buongiorno model. J Magn Magn Mater. 2016;416:164–73. https://doi.org/10.1016/j.jmmm.2016.05.026.
[52] Buongiorno J. Convective transport in nanofluids. J Heat Transfer. 2006;128:240–50.
[53] Sheikholeslami M, Rashidi MM, Al Saad DM, Firouzi F, Rokni HB, Domairry G. Steady nanofluid flow between parallel plates considering thermophoresis and Brownian effects. J King Saud Univ - Sci. 2016;28:380–9.
[54] Milani Shirvan K, Mamourian M, Mirzakhanlari S, Ellahi R. Two phase simulation and sensitivity analysis of effective parameters on combined heat transfer and pressure drop in a solar heat exchanger filled with nanofluid by RSM. J Mol Liq. 2016;220:888–901.
[55] Rahimi-Gorji M, Pourmehran O, Gorji-Bandpy M, Ganji DD. Unsteady squeezing nanofluid simulation and investigation of its effect on important heat transfer parameters in presence of magnetic field. J Taiwan Inst Chem Eng. 2016;67:467–75.
[56] Mahmoodi M, Kandelousi S. Application of DTM for kerosene-alumina nanofluid flow and heat transfer between two rotating plates. Eur Phys J Plus. 2015;130:142.
[57] Khan U, Ahmed N, Mohyud-Din ST. Analysis of magnetohydrodynamic flow and heat transfer of Cu–water nanofluid between parallel plates for different shapes of nanoparticles. Neural Comput Applic. 2016. https://doi.org/10.1007/s00521-016-2596-x.
[58] Mosayebidorcheh S, Sheikholeslami M, Hatami M, Ganji DD. Analysis of turbulent MHD Couette nanofluid flow and heat transfer using hybrid DTM–FDM. Particuology. 2016;26:95–101.
[59] Sheikholeslami M, Hatami M, Ganji DD. Nanofluid flow and heat transfer in a rotating system in the presence of a magnetic field. J Mol Liq. 2014;190:112–20.
[60] Liao S. Homotopy analysis method in nonlinear differential equations Springer Science & Business Media ; 2012.
[61] Mahmoodi M, Kandelousi S. Cooling process of liquid propellant rocket by means of kerosene-alumina nanofluid. Propuls Power Res. 2016;5:279–86.
[62] Mahmoodi M, Kandelousi S. Semi-analytical investigation of kerosene-alumina nanofluid between two parallel plates. J Aerosp Eng. 2016;29:04016001.
[63] Sheikholeslami M, Abelman S, Ganji DD. Numerical simulation of MHD nanofluid flow and heat transfer considering viscous dissipation. Int J Heat Mass Transf. 2014;79:212–22.
[64] Öztürk A, Kahveci K. Slip flow of nanofluids between parallel plates heated with a constant heat flux. Strojniški Vestn - J Mech Eng. 2016;62:511–20.
[65] Mohyud-Din ST, Zaidi ZA, Khan U, Ahmed N. On heat and mass transfer analysis for the flow of a nanofluid between rotating parallel plates. Aerosp Sci Technol. 2015;46:514–22.
[66] Singh K, Rawat SK, Kumar M. Heat and mass transfer on squeezing unsteady MHD nanofluid flow between parallel plates with slip velocity effect. J Nanosci. 2016;2016:1–11.
[67] Hatami M, Jing D. Differential transformation method for Newtonian and non-Newtonian nanofluids flow analysis: compared to numerical solution. Alex Eng J. 2016;55:731–9.
[68] Aly EH, Sayed HM. A comparative study of five nanofluids for heat transfer of squeezing and unsteady flow between two parallel plates with Vogel's model of viscosity. J Comput Theor Nanosci. 2016;13:3097–104.
[69] Domairry G, Hatami M. Squeezing Cu–water nanofluid flow analysis between parallel plates by DTM-Padé method. J Mol Liq. 2014;193:37–44.
[70] Dogonchi AS, Divsalar K, Ganji DD. Flow and heat transfer of MHD nanofluid between parallel plates in the presence of thermal radiation. Comput Methods Appl Mech Eng. 2016;310:58–76.

[71] Haq R, Hammouch Z, Khan W. Water-based squeezing flow in the presence of carbon nanotubes between two parallel disks. Therm Sci. 2016;20:1973–81.
[72] Hayat T, Muhammad K, Farooq M, Alsaedi A. Unsteady squeezing flow of carbon nanotubes with convective boundary conditions. PLoS One. 2016;11:e0152923.
[73] Acharya N, Das K, Kundu PK. The squeezing flow of Cu-water and Cu-kerosene nanofluids between two parallel plates. Alex Eng J. 2016;55:1177–86.
[74] Azimi M, Riazi R. Analytical solution of unsteady GO-water nanofluid flow and heat transfer between two parallel moving plates. Indian J Chem Technol. 2016;23:47–52.
[75] Pourmehran O, Rahimi-Gorji M, Gorji-Bandpy M, Ganji DD. Analytical investigation of squeezing unsteady nanofluid flow between parallel plates by LSM and CM. Alex Eng J. 2015;54:17–26.
[76] Azimi A, Mirzaei M. Analytical investigation of squeezing flow of graphene oxide water nanofluid between parallel plates using RVIM. J Comput Theor Nanosci. 2015;12:175–9.
[77] Dib A, Haiahem A, Bou-said B. Approximate analytical solution of squeezing unsteady nanofluid flow. Powder Technol. 2015;269:193–9.
[78] Azimi M, Azimi A, Mirzaei M. Investigation of the unsteady graphene oxide nanofluid flow between two moving plates. J Comput Theor Nanosci. 2014;11:2104–8.
[79] Huang X-J, Vafai K, Li Y-R. Nanofluid buoyancy-driven heat transfer in three-dimensional horizontal annuli. Eur J Mech - B/Fluids. 2020;82:66–82. https://doi.org/10.1016/j.euromechflu.2020.02.005.
[80] Abbassi Y, Shirani AS, Asgarian S. Two-phase mixture simulation of Al2O3/water nanofluid heat transfer in a non-uniform heat addition test section. Prog Nucl Energy. 2015;83:356–64.
[81] Abbasian Arani AA, Aberoumand H, Aberoumand S, Jafari Moghaddam A, Dastanian M. An empirical investigation on thermal characteristics and pressure drop of Ag-oil nanofluid in concentric annular tube. Heat Mass Transf. 2016;52:1693–706.
[82] Jafarimoghaddam A, Aberoumand S. An empirical investigation on Cu/ethylene glycol nanofluid through a concentric annular tube and proposing a correlation for predicting Nusselt number. Alex Eng J. 2016;55:1047–52.
[83] Khajeh Arzani H, Amiri A, Kazi SN, Chew BT, Badarudin A. Experimental investigation of thermophysical properties and heat transfer rate of covalently functionalized MWCNT in an annular heat exchanger. Int Commun Heat Mass Transf. 2016;75:67–77.
[84] Khajeh Arzani H, Amiri A, Arzani HK, Bin Rozali S, Kazi SN, Badarudin A. Toward improved heat transfer performance of annular heat exchangers with water/ethylene glycol-based nanofluids containing graphene nanoplatelets. J Therm Anal Calorim. 2016;126:1427–36.
[85] Khajeh Arzani H, Amiri A, Kazi SN, Chew BT, Badarudin A. Experimental and numerical investigation of thermophysical properties, heat transfer and pressure drop of covalent and noncovalent functionalized graphene nanoplatelet-based water nanofluids in an annular heat exchanger. Int Commun Heat Mass Transf. 2015;68:267–75.
[86] Abbassi Y, Talebi M, Shirani AS, Khorsandi J. Experimental investigation of TiO2/water nanofluid effects on heat transfer characteristics of a vertical annulus with non-uniform heat flux in non-radiation environment. Ann Nucl Energy. 2014;69:7–13.
[87] Aljabair S, Mohammed AA, Alesbe I. Natural convection heat transfer in corrugated annuli with H2O-Al2O3 nanofluid. Heliyon. 2020;6:e05568. https://doi.org/10.1016/j.heliyon.2020.e05568.
[88] Sheikholeslami M, Ganji DD. Nanofluid flow and heat transfer between parallel plates considering Brownian motion using DTM. Comput Methods Appl Mech Eng. 2015;283:651–63.
[89] Malvandi A, Ganji DD. Magnetic field and slip effects on free convection inside a vertical enclosure filled with alumina/water nanofluid. Chem Eng Res Des. 2015;94:355–64.
[90] Godson L, Raja B, Mohan Lal D, Wongwises S. Enhancement of heat transfer using nanofluids—an overview. Renew Sustain Energy Rev. 2010;14:629–41. https://doi.org/10.1016/j.rser.2009.10.004.
[91] Özerinç S, Kakaç S, Yazıcıoğlu AG. Enhanced thermal conductivity of nanofluids: a state-of-the-art review. Microfluid Nanofluid. 2010;8:145–70.
[92] Philip J, Shima PD, Raj B. Evidence for enhanced thermal conduction through percolating structures in nanofluids. Nanotechnology. 2008;19:1–7. https://doi.org/10.1088/0957-4484/19/30/305706.
[93] Philip J, Shima PD, Raj B. Enhancement of thermal conductivity in magnetite based nanofluid due to chainlike structures. Appl Phys Lett. 2007;91:203108.
[94] Philip J, Shima PD, Raj B. Nanofluid with tunable thermal properties. Appl Phys Lett. 2008;92. https://doi.org/10.1063/1.2838304.
[95] Prasher R, Evans W, Meakin P, Fish J, Phelan P, Keblinski P. Effect of aggregation on thermal conduction in colloidal nanofluids. Appl Phys Lett. 2006;89. https://doi.org/10.1063/1.2360229.
[96] Sheikholeslami M, Ganji DD. Numerical investigation for two phase modeling of nanofluid in a rotating system with permeable sheet. J Mol Liq. 2014;194:13–9.
[97] Sheikholeslami M, Ganji DD. Three dimensional heat and mass transfer in a rotating system using nanofluid. Powder Technol. 2014;253:789–96.
[98] Sheikholeslami M, Domiri Ganji D, Younus Javed M, Ellahi R. Effect of thermal radiation on magnetohydrodynamics nanofluid flow and heat transfer by means of two phase model. J Magn Magn Mater. 2015;374:36–43.
[99] Sheikholeslami M, Rokni HB. Nanofluid two phase model analysis in existence of induced magnetic field. Int J Heat Mass Transf. 2017;107:288–99.
[100] Sheikholeslami M, Ganji DD. Nanofluid hydrothermal behavior in existence of Lorentz forces considering joule heating effect. J Mol Liq. 2016;224:526–37.
[101] Shah Z, Gul T, Islam S, Khan MA, Bonyah E, Hussain F, et al. Three dimensional third grade nanofluid flow in a rotating system between parallel plates with Brownian motion and thermophoresis effects. Results Phys. 2018;10:36–45. https://doi.org/10.1016/j.rinp.2018.05.020.
[102] Yang C, Wu X, Zheng Y, Qiu T. Heat transfer performance assessment of hybrid nanofluids in a parallel channel under identical pumping power. Chem Eng Sci. 2017;168:67–77. https://doi.org/10.1016/j.ces.2017.04.045.
[103] Zhu J, Yang D, Zheng L, Zhang X. Effects of second order velocity slip and nanoparticles migration on flow of Buongiorno nanofluid. Appl Math Lett. 2016;52:183–91.
[104] Hatami M, Jing D, Song D, Sheikholeslami M, Ganji DD. Heat transfer and flow analysis of nanofluid flow between parallel plates in presence of variable magnetic field using HPM. J Magn Magn Mater. 2015;396:275–82.
[105] Hatami M, Ganji DD. Heat transfer and nanofluid flow in suction and blowing process between parallel disks in presence of variable magnetic field. J Mol Liq. 2014;190:159–68.
[106] Hayat T, Muhammad T, Qayyum A, Alsaedi A, Mustafa M. On squeezing flow of nanofluid in the presence of magnetic field effects. J Mol Liq. 2016;213:179–85.
[107] Hayat T, Abbas T, Ayub M, Muhammad T, Alsaedi A. On squeezed flow of Jeffrey Nanofluid between two parallel disks. Appl Sci. 2016;6:346.
[108] Mohyud-Din ST, Khan SIU, Darus M, Hassan SM. Unsteady mixed convection squeezing flow of nanofluid between parallel disks. Adv Mech Eng. 2016;8:1–13.
[109] Azimi M, Riazi R. MHD unsteady GO–water-squeezing nanofluid flow—heat and mass transfer between two infinite parallel moving plates: analytical investigation. Sadhana - Acad Proc Eng Sci. 2017;42:335–41.
[110] Azimi M, Riazi R. Heat transfer analysis of GO-water nanofluid flow between two parallel disks. Propul Power Res. 2015;4:23–30.
[111] Malvandi A, Ganji DD. Mixed convection of alumina–water nanofluid inside a concentric annulus considering nanoparticle migration. Particuology. 2016;24:113–22.
[112] Zamani M, Malvandi A, Moshizi SA, Hosseini SJ. Nanofluid flow in micro-annular tubes at constant wall temperature considering the non-uniform distribution of nanoparticles. Eur J Mech - B/Fluids. 2017. https://doi.org/10.1016/j.euromechflu.2017.03.006.
[113] Yang C, Li W, Nakayama A. Convective heat transfer of nanofluids in a concentric annulus. Int J Therm Sci. 2013;71:249–57. https://doi.org/10.1016/j.ijthermalsci.2013.04.007.
[114] Hu Y-P, Li Y-R, Lu L, Mao Y-J, Li M-H. Natural convection of water-based nanofluids near the density maximum in an annulus. Int J Therm Sci. 2020;152:106309. https://doi.org/10.1016/j.ijthermalsci.2020.106309.
[115] Horng HE, Chen CS, Fang KL, Yang SY, Chieh JJ, Hong C-Y, et al. Tunable optical switch using magnetic fluids. Appl Phys Lett. 2004;85:5592–4. https://doi.org/10.1063/1.1833564.
[116] Hergt R, Dutz S, Müller R, Zeisberger M. Magnetic particle hyperthermia: nanoparticle magnetism and materials development for cancer therapy. J Phys Condens Matter. 2006;18:S2919–34. https://doi.org/10.1088/0953-8984/18/38/S26.
[117] Liu C-T, Kumakura T, Ishikawa K, Hashizume H, Takeda K, Ito M, et al. Effects of assisted magnetic field to an atmospheric-pressure plasma jet on radical generation at the plasma-surface interface and bactericidal function. Plasma Sour Sci Technol. 2016;25:065005. https://doi.org/10.1088/0963-0252/25/6/065005.
[118] Mirshahghassemi S, Lead JR. Oil recovery from water under environmentally relevant conditions using magnetic nanoparticles. Environ Sci Technol. 2015;49:11729–36. https://doi.org/10.1021/acs.est.5b02687.
[119] Kalavathi GK, Dinesh PA, Gururajan K. Numerical study of magnetic field on rough porous narrow journal bearing with heterogeneous surface. Mater Today Proc. 2017;4:10539–43. https://doi.org/10.1016/j.matpr.2017.06.416.
[120] Xinghe Fu, Jibin Zou. Numerical analysis on the magnetic field of hybrid exciting synchronous generator. IEEE Trans Magn. 2009;45:4590–3. https://doi.org/10.1109/TMAG.2009.2023625.
[121] Peng Y, Zhao L, Song S, Sha C, Li R, Xu Y. Experimental study on alternating magnetic field magnetohydrodynamic pump. J Hydrodyn Ser B. 2008;20:591–5. https://doi.org/10.1016/S1001-6058(08)60099-2.
[122] Rokni HB, Alsaad DM, Valipour P. Electrohydrodynamic nanofluid flow and heat transfer between two plates. J Mol Liq. 2016;216:583–9.
[123] Ali AO, Makinde OD, Nkansah-Gyekye Y. Numerical study of unsteady MHD Couette flow and heat transfer of nanofluids in a rotating system with convective cooling. Int J Numer Methods Heat Fluid Flow. 2016;26:1567–79.
[124] Selimefendigil F, Öztop HF. MHD pulsating forced convection of nanofluid over parallel plates with blocks in a channel. Int J Mech Sci. 2019;157–158:726–40. https://doi.org/10.1016/j.ijmecsci.2019.04.048.
[125] Amani P, Amani M, Mehrali M, Vajravelu K. Influence of quadrupole magnetic field on mass transfer in an extraction column in the presence of MnFe2O4 nanoparticles. J Mol Liq. 2017;238:145–54.
[126] Amani M, Amani P, Kasaeian A, Mahian O, Pop I, Wongwises S. Modeling and optimization of thermal conductivity and viscosity of MnFe2O4 nanofluid under magnetic field using an ANN. Sci Rep. 2017;7:17369. https://doi.org/10.1038/s41598-017-17444-5.
[127] Amani M, Amani P, Kasaeian A, Mahian O, Wongwises S. Thermal conductivity measurement of spinel-type ferrite MnFe2O4 nanofluids in the presence of a uniform magnetic field. J Mol Liq. 2017;230:121–8. https://doi.org/10.1016/j.molliq.2016.12.013.
[128] Amani M, Amani P, Kasaeian A, Mahian O, Kasaeian F, Wongwises S. Experimental study on viscosity of spinel-type manganese ferrite nanofluid in attendance of magnetic field. J Magn Magn Mater. 2017;428:457–63. https://doi.org/10.1016/j.jmmm.2016.12.129.
[129] Das K, Jana S, Acharya N. Slip effects on squeezing flow of nanofluid between two parallel disks. Int J Appl Mech Eng. 2016;21:5–20.
[130] Hayat T, Khan M, Imtiaz M, Alsaedi A. Squeezing flow past a Riga plate with chemical reaction and convective conditions. J Mol Liq. 2017;225:569–76.

[131] Kandasamy R, Mohammad R, Zailani NABM, Jaafar NFB. Nanoparticle shapes on squeezed MHD nanofluid flow over a porous sensor surface. J Mol Liq. 2017;233: 156–65.
[132] Kandasamy R, Adnan NA Bt, Mohammad R. Nanoparticle shape effects on squeezed MHD flow of water based Cu, Al 2 O 3 and SWCNTs over a porous sensor surface. Alex Eng J. 2018;57(3):1433–45.
[133] Hedayati N, Ramiar A. Investigation of two phase unsteady nanofluid flow and heat transfer between moving parallel plates in the presence of the magnetic field using GM. Trans Phenom Nano Micro Scales. 2016;4:52–8.
[134] Sheikholeslami M, Hatami M, Domairry G. Numerical simulation of two phase unsteady nanofluid flow and heat transfer between parallel plates in presence of time dependent magnetic field. J Taiwan Inst Chem Eng. 2015;46:43–50.
[135] Rizwan-ul-Haq ZH, Khan ST, Hussain Z Hammouch. Flow and heat transfer analysis of water and ethylene glycol based Cu nanoparticles between two parallel disks with suction/injection effects. J Mol Liq. 2016;221:298–304.
[136] Sheikholeslami M, Nimafar M, Ganji DD. Nanofluid heat transfer between two pipes considering Brownian motion using AGM. Alex Eng J. 2017. https://doi.org/10.1016/j.aej.2017.01.032.
[137] Malvandi A, Safaei MR, Kaffash MH, Ganji DD. MHD mixed convection in a vertical annulus filled with Al2O3–water nanofluid considering nanoparticle migration. J Magn Magn Mater. 2015;382:296–306.
[138] Selimefendigil F, Öztop HF. Conjugate natural convection in a nanofluid filled partitioned horizontal annulus formed by two isothermal cylinder surfaces under magnetic field. Int J Heat Mass Transf. 2017;108:156–71.
[139] Abbas Z, Hasnain J. Two-phase magnetoconvection flow of magnetite (Fe3O4) nanoparticles in a horizontal composite porous annulus. Results Phys. 2017;7: 574–80.
[140] Bahiraei M, Hosseinalipour SM, Hangi M, Mostafa S. Numerical study and optimization of hydrothermal characteristics of Mn–Zn ferrite nanofluid within annulus in the presence of magnetic field. J Supercond Nov Magn. 2014;27:527–34.
[141] Sheikholeslami M, Jalili P, Ganji DD. Magnetic field effect on nanofluid flow between two circular cylinders using AGM. Alex Eng J. 2017. https://doi.org/10.1016/j.aej.2017.02.010.
[142] Moshizi SA, Pop I. Conjugated effect of joule heating and magnetohydrodynamic on laminar convective heat transfer of nanofluids inside a concentric annulus in the presence of slip condition. Int J Thermophys. 2016;37:72.
[143] Malvandi A, Moshizi SA, Ganji DD. Effect of magnetic fields on heat convection inside a concentric annulus filled with Al2O3–water nanofluid. Adv Powder Technol. 2014;25:1817–24.
[144] Malvandi A, Ghasemi A, Ganji DD. Thermal performance analysis of hydromagnetic Al2O3-water nanofluid flows inside a concentric microannulus considering nanoparticle migration and asymmetric heating. Int J Therm Sci. 2016;109:10–22.
[145] Malvandi A, Moshizi SA, Ganji DD. Nanoparticle transport effect on magnetohydrodynamic mixed convection of electrically conductive nanofluids in micro-annuli with temperature-dependent thermophysical properties. Phys E Low-Dimension Syst Nanostruct. 2017;88:35–49. https://doi.org/10.1016/j.physe.2016.10.043.
[146] Aboud ED, Rashid HK, Jassim HM, Ahmed SY, Waheed Khafaji SO, Hamzah HK, et al. MHD effect on mixed convection of annulus circular enclosure filled with Non-Newtonian nanofluid. Heliyon. 2020;6:e03773. https://doi.org/10.1016/j.heliyon.2020.e03773.
[147] Dalvi S, Karaliolios ECJ, van der Meer TH, Shahi M. Thermo-magnetic convection in a circular annulus filled with magnetocaloric nanofluid. Int Commun Heat Mass Transf. 2020;116:104654. https://doi.org/10.1016/j.icheatmasstransfer.2020.104654.
[148] Dogonchi AS, Hashim. Heat transfer by natural convection of Fe3O4-water nanofluid in an annulus between a wavy circular cylinder and a rhombus. Int J Heat Mass Transf. 2019;130:320–32. https://doi.org/10.1016/j.ijheatmasstransfer.2018.10.086.
[149] Bahiraei M, Hosseinalipour SM, Hangi M. Heat transfer and flow characteristics of nanofluid in a narrow annulus: numerical study, modelling and optimisation. Can J Chem Eng. 2014;92:747–57.
[150] Alawi OA, Che Sidik NA, Dawood HK. Numerical study of turbulent mixed convection of nanofluids in three-dimensional horizontal concentric annuli. J Comput Theor Nanosci. 2015;12:2067–76.
[151] Togun H, Kazi SN, Badarudin A. Turbulent heat transfer to separation nanofluid flow in annular concentric pipe. Int J Therm Sci. 2017;117:14–25.
[152] Togun H, Abu-Mulaweh HI, Kazi SN, Badarudin A. Numerical simulation of heat transfer and separation Al 2 O 3/nanofluid flow in concentric annular pipe. Int Commun Heat Mass Transf. 2016;71:108–17.
[153] Peña NLC, Rivera-Solorio CI, Payán-Rodríguez LA, García-Cuéllar AJ, López-Salinas JL. Experimental analysis of natural convection in vertical annuli filled with AlN and TiO2/mineral oil-based nanofluids. Int J Therm Sci. 2017;111:138–45.
[154] Turkyilmazoglu M. Anomalous heat transfer enhancement by slip due to nanofluids in circular concentric pipes. Int J Heat Mass Transf. 2015;85:609–14.
[155] Seyyedi SM, Dayyan M, Soleimani S, Ghasemi E. Natural convection heat transfer under constant heat flux wall in a nanofluid filled annulus enclosure. Ain Shams Eng J. 2015;6:267–80.
[156] Fallah K, Ghaderi A, Sedaghatizadeh N, Borghei MH. Simulation of natural convection heat transfer using nanofluid in a concentric annulus. Therm Sci. 2017;21(3): 1275–86.
[157] Mirzaie M, Lakzian E. Natural convection of Cu–water nanofluid near water density inversion in horizontal annulus with different arrangements of discrete heat source – sink pair. Adv Powder Technol. 2016;27:1337–46.
[158] Sheremet MA, Pop I. Natural convection in a horizontal cylindrical annulus filled with a porous medium saturated by a nanofluid using Tiwari and Das' nanofluid model. Eur Phys J Plus. 2015;130:107.
[159] Pourmirzaagha H, Hassanzadeh Afrouzi H, Abouei Mehrizi A. Nano-particles transport in a concentric annulus: a lattice Boltzmann approach. J Theor Appl Mech. 2015;53:683.
[160] Zhang C, Zheng L, Jiang Y, Zhang X. Unsteady natural convection heat transfer of nanofluid in an annulus with a sinusoidally heated source. Numer Heat Transf Part A Appl. 2016;69:97–108.
[161] Sheikholeslami M, Ganji DD. Unsteady nanofluid flow and heat transfer in presence of magnetic field considering thermal radiation. J Br Soc Mech Sci Eng. 2015;37: 895–902.
[162] Hayat T, Sajjad R, Alsaedi A, Muhammad T, Ellahi R. On squeezed flow of couple stress nanofluid between two parallel plates. Results Phys. 2017;7:553–61.
[163] Gupta AK, Saha Ray S. Numerical treatment for investigation of squeezing unsteady nanofluid flow between two parallel plates. Powder Technol. 2015;279:282–9.
[164] Thompson P, Troian S. A general boundary condition for liquid flow at solid surfaces. Nature. 1997;289:360–2.
[165] Malvandi A, Moshizi SA, Soltani EG, Ganji DD. Modified Buongiorno's model for fully developed mixed convection flow of nanofluids in a vertical annular pipe. Comput Fluids. 2014;89:124–32.
[166] Rashidi MM, Reza M, Gupta S. MHD stagnation point flow of micropolar nanofluid between parallel porous plates with uniform blowing. Powder Technol. 2016;301: 876–85.
[167] Hashmi MM, Hayat T, Alsaedi A. On the analytic solutions for squeezing flow of nanofluid between parallel disks. Nonlinear Anal Model Control. 2012;17:418–30.
[168] Moshizi SA, Malvandi A. Different modes of nanoparticle migration at mixed convection of Al2O3–water nanofluid inside a vertical microannulus in the presence of heat generation/absorption. J Therm Anal Calorim. 2016;126:1947–62.
[169] Moshizi SA, Malvandi A, Ganji DD, Pop I. A two-phase theoretical study of Al2O3–water nanofluid flow inside a concentric pipe with heat generation/absorption. Int J Therm Sci. 2014;84:347–57.
[170] Bouzerzour A, Djezzar M, Oztop HF, Tayebi T, Abu-Hamdeh N. Natural convection in nanofluid filled and partially heated annulus: effect of different arrangements of heaters. Phys A Stat Mech Its Appl. 2020;538:122479. https://doi.org/10.1016/j.physa.2019.122479.
[171] Sahebi SAR, Pourziaei H, Feizi AR, Taheri MH, Rostamiyan Y, Ganji DD. Numerical analysis of natural convection for non-Newtonian fluid conveying nanoparticles between two vertical parallel plates. Eur Phys J Plus. 2015;130:238.
[172] Hatami M, Ganji DD. Natural convection of sodium alginate (SA) non-Newtonian nanofluid flow between two vertical flat plates by analytical and numerical methods. Case Stud Therm Eng. 2014;2:14–22.
[173] Bahiraei M, Alighardashi M. Investigating non-Newtonian nanofluid flow in a narrow annulus based on second law of thermodynamics. J Mol Liq. 2016;219:117–27.
[174] Tayebi T, Öztop HF, Chamkha AJ. Natural convection and entropy production in hybrid nanofluid filled-annular elliptical cavity with internal heat generation or absorption. Therm Sci Eng Prog. 2020;19:100605. https://doi.org/10.1016/j.tsep.2020.100605.
[175] Shah NA, Seikh AH, Tlili I, Shah K, Shabbir RM, Rahimi-Gorji M, et al. Natural convection of bio-nanofluid between two vertical parallel plates with damped shear and thermal flux. J Mol Liq. 2019;296:111575. https://doi.org/10.1016/j.molliq.2019.111575.
[176] Selimefendigil F, Öztop HF. Impacts of rotating surface and oriented magnetic field on mixed convection and melting behavior of CNT-water nanouid in a horizontal annulus. Int Commun Heat Mass Transf. 2021;120:104935. https://doi.org/10.1016/j.icheatmasstransfer.2020.104935.
[177] Ikram MD, Asjad MI, Akgül A, Baleanu D. Effects of hybrid nanofluid on novel fractional model of heat transfer flow between two parallel plates. Alex Eng J. 2021;60: 3593–604. https://doi.org/10.1016/j.aej.2021.01.054.
[178] Tayebi T, Öztop HF. Entropy production during natural convection of hybrid nanofluid in an annular passage between horizontal confocal elliptic cylinders. Int J Mech Sci. 2020;171:105378. https://doi.org/10.1016/j.ijmecsci.2019.105378.
[179] Siavashi M, Talesh Bahrami HR, Saffari H. Numerical investigation of flow characteristics, heat transfer and entropy generation of nanofluid flow inside an annular pipe partially or completely filled with porous media using two-phase mixture model. Energy. 2015;93:2451–66.
[180] Mashaei PR, Shahryari M, Madani S. Numerical hydrothermal analysis of water-Al2O3 nanofluid forced convection in a narrow annulus filled by porous medium considering variable properties. J Therm Anal Calorim. 2016;126:891–904.
[181] Miles A, Bessaïh R. Heat transfer and entropy generation analysis of three-dimensional nanofluids flow in a cylindrical annulus filled with porous media. Int Commun Heat Mass Transf. 2021;124:105240. https://doi.org/10.1016/j.icheatmasstransfer.2021.105240.
[182] El-Maghlany WM, Hanafy AA, Hassan AA, El-Magid MA. Experimental study of cu–water nanofluid heat transfer and pressure drop in a horizontal double-tube heat exchanger. Exp Therm Fluid Sci. 2016;78:100–11.
[183] Malvandi A, Ganji DD. Effects of nanoparticle migration on water/alumina nanofluid flow inside a horizontal annulus with a moving core. J Mech Des. 2015;31:291–305.
[184] Yekani Motlagh S, Golab E, Sadr AN. Two-phase modeling of the free convection of nanofluid inside the inclined porous semi-annulus enclosure. Int J Mech Sci. 2019; 164:105183. https://doi.org/10.1016/j.ijmecsci.2019.105183.
[185] Siavashi M, Rostami A. Two-phase simulation of non-Newtonian nanofluid natural convection in a circular annulus partially or completely filled with porous media. Int J Mech Sci. 2017;133:689–703. https://doi.org/10.1016/j.ijmecsci.2017.09.031.
[186] Rezaei Gorjaei A, Soltani M, Bahiraei M, Kashkooli FM. CFD simulation of nanofluid forced convection inside a three-dimensional annulus by two-phase mixture approach: heat transfer and entropy generation analyses. Int J Mech Sci. 2018; 146–147:396–404. https://doi.org/10.1016/j.ijmecsci.2018.08.002.

[187] Jourabian M, Rabienataj Darzi AA, Akbari OA, Toghraie D. The enthalpy-based lattice Boltzmann method (LBM) for simulation of NePCM melting in inclined elliptical annulus. Phys A Stat Mech Its Appl. 2020;548:123887. https://doi.org/10.1016/j.physa.2019.123887.
[188] Ashraf MA, Liu Z, Li C, Yang Y, Ross D. MRT lattice Boltzmann simulation of free convection in a symmetrical annulus combined with experimental data of TiO2-H2O nanofluid's properties. Powder Technol. 2020;362:717–28. https://doi.org/10.1016/j.powtec.2019.12.036.
[189] Usman M, Zubair T, Hamid M, Haq RU. Novel modification in wavelets method to analyze unsteady flow of nanofluid between two infinitely parallel plates. Chinese J Phys. 2020;66:222–36. https://doi.org/10.1016/j.cjph.2020.03.031.
[190] Siavashi M, Jamali M. Heat transfer and entropy generation analysis of turbulent flow of TiO2-water nanofluid inside annuli with different radius ratios using two-phase mixture model. Appl Therm Eng. 2016;100:1149–60.
[191] Rohsenow W, Hartnett J, Cho Y. Handbook of heat transfer. McGraw-Hill New York; 1998.
[192] Mokhtari Moghari R, Talebi F, Rafee R, Shariat M. Numerical study of pressure drop and thermal characteristics of Al2O3–water nanofluid flow in horizontal annuli. Heat Transf Eng. 2015;36:166–77.
[193] Imani H, Cheraqi A, Jafarian A, Heyhat MM. Numerical simulation of Al2O3–water nanofluid mixed convection in an inclined annulus. Energy Equip Syst. 2015;3:97–111.
[194] Izadi M, Behzadmehr A, Shahmardan MM. Effects of inclination angle on laminar mixed convection of a nanofluid flowing through an annulus. Chem Eng Commun. 2015;202:1693–702.